SPECTRAL APPROXIMATION OF ELLIPTIC OPERATORS BY THE HYBRID HIGH-ORDER METHOD

VICTOR CALO, MATTEO CICUTTIN, QUANLING DENG, AND ALEXANDRE ERN

ABSTRACT. We study the approximation of the spectrum of a second-order elliptic differential operator by the Hybrid High-Order (HHO) method. The HHO method is formulated using cell and face unknowns which are polynomials of some degree $k \geq 0$. The key idea for the discrete eigenvalue problem is to introduce a discrete operator where the face unknowns have been eliminated. Using the abstract theory of spectral approximation of compact operators in Hilbert spaces, we prove that the eigenvalues converge as h^{2t} and the eigenfunctions as h^t in the H^1-seminorm, where h is the mesh-size, $t \in [s, k+1]$ depends on the smoothness of the eigenfunctions, and $s > \frac{1}{2}$ results from the elliptic regularity theory. The convergence rates for smooth eigenfunctions are thus h^{2k+2} for the eigenvalues and h^{k+1} for the eigenfunctions. Our theoretical findings, which improve recent error estimates for Hybridizable Discontinuous Galerkin (HDG) methods, are verified on various numerical examples including smooth and non-smooth eigenfunctions. Moreover, we observe numerically in one dimension for smooth eigenfunctions that the eigenvalues superconverge as h^{2k+4} for a specific value of the stabilization parameter.

1. INTRODUCTION

The Hybrid High-Order (HHO) method has been recently introduced for diffusion problems in [28] and for linear elasticity problems in [27]. The HHO method is formulated by introducing cell and face unknowns which are polynomials of some degree $k \geq 0$ (some variations in the degree of the cell unknowns are possible; see [17]). The method is then devised from a local reconstruction operator and a (subtle) local stabilization operator in each mesh cell. This leads to a discretization method that supports general meshes (with polyhedral cells and non-matching interfaces). Moreover, when approximating smooth solutions of second-order elliptic source problems, the method delivers error estimates of order h^{k+1} in the H^1-seminorm and of order h^{k+2} in the L^2-norm under full elliptic regularity. Positioning unknowns at the mesh faces is also a natural way to express locally in each mesh cell the balance properties satisfied by the model problem. As shown in [17], the HHO method can be fitted into the family of Hybridizable Discontinuous Galerkin (HDG) methods introduced in [18] (and thus to the Weak Galerkin method [47]) and is also closely related to the non-conforming Virtual Element

Method from [5]. The HHO method has undergone a vigorous development over the last few years; we mention, among others, the application to advection-diffusion equations in [25], to the Stokes equations in [29], to the Leray–Lions equations in [24], and to hyperelasticity with finite deformations in [1]. The implementation of HHO methods is described in [16]. As already pointed out in [27, 28], the cell unknowns can be eliminated locally in each mesh cell, leading to a global Schur complement problem with compact stencil in terms of the face unknowns.

The goal of this work is to devise and analyze HHO methods for the discretization of the eigenvalue problem associated with a second-order elliptic differential operator. There are several salient motivations for considering HHO methods for the present problem. First, HHO methods support general meshes with polyhedral cells and hanging nodes resulting, e.g., from the presence of non-matching interfaces. An example on general meshes is presented in the numerical experiments below. Second, HHO methods do not require tunable parameters, as opposed to Interior Penalty Discontinuous Galerkin methods for instance, where the penalty parameter depends in particular on the value of a certain constant in a discrete trace inequality. Third, HHO methods are computationally effective since (i) they are based on the primal formulation and do not require to introduce dual variables, (ii) they lead to face-based stencils that are (far) more compact than vertex-based stencils (especially in 3D) as produced by conforming finite element methods for instance, and (iii) because HHO methods attach degrees of freedom to the mesh faces, the size of the problem grows quadratically with the polynomial degree instead of cubically as in discontinuous Galerkin methods.

The key idea in the analysis of the HHO approximation of the eigenvalue problem is to formulate the discrete problem by letting the mass bilinear form act only on the cell unknowns, whereas the stiffness bilinear form acts, as for the discrete source problem, on both cell and face unknowns. Thus, the first main contribution of this work is to identify the relevant HHO solution operator approximating the exact solution operator. We show that this can be achieved by introducing a purely cell-based operator, where the face unknowns have been eliminated by expressing them in terms of the cell unknowns. Note that the elimination process is reversed with respect to the usual approach for the source problem, where one ends up with a face-based discrete operator. While the present cell-based operator is not needed for actual computations, it plays a central role in the error analysis. Indeed, with this tool in hand, it becomes possible to analyze the approximation error on the eigenvalues and the eigenfunctions by means of the abstract theory of spectral approximation of compact operators in Hilbert spaces following the work of Vaĭnikko [45, 46], Bramble and Osborn [10, 41], Descloux et al. [22, 23], and Babuška and Osborn [6]. The second main contribution of this work is Theorem 4.4 and Corollary 4.6 which establish a convergence of order h^{2t} for the eigenvalues and of order h^t for the eigenfunctions in the H^1-seminorm, where $t \in [s, k+1]$ is the smoothness index related to the eigenfunctions and $s \in (\frac{1}{2}, 1]$ is the smoothness index resulting from the elliptic regularity theory. In the case of smooth eigenfunctions, we have $t = k+1$, leading to a convergence of order h^{2k+2} for the eigenvalues and of order h^{k+1} for the eigenfunctions in the H^1-seminorm. These convergence orders are confirmed by our numerical experiments including both smooth and non-smooth eigenfunctions of the Laplace operator in one and two dimensions. We highlight

that these convergence results are so far lacking for HDG methods (see the discussion in the next paragraph), so that the present work contributes to fill this gap. Finally, the third contribution of this work is the numerical observation of a superconvergence of order h^{2k+4} for the eigenvalues in one dimension whenever the stabilization parameter is chosen to be equal to $(2k+3)$.

Let us put our results in perspective with the literature on the approximation of elliptic eigenvalue problems by other discretization methods. Following the early work in [44], it is well known that using H^1-conforming finite elements of degree $k \geq 1$ on simplicial meshes leads to convergence rates of order h^{2k} for the eigenvalues and of order h^k for the eigenfunctions (provided the eigenfunctions are smooth enough). We refer the reader to [8] for a review on the finite element approximation of eigenvalue problems. Similar results were obtained more recently in [3, 33] for discontinuous Galerkin (dG) methods. The analysis of the spectral approximation by mixed and mixed-hybrid methods was started in [14, 38, 39] and expanded in [9, 30]. Hybridization techniques leading to an eigenproblem on the face unknowns were studied in [19] for Raviart–Thomas mixed finite elements; therein, it was also observed that the use of a local post-processing technique improves the accuracy of the computed eigenfunctions (see also [31] for the lowest-order case). The approximation of elliptic eigenvalue problems using the Virtual Element Method (VEM) was studied in [32], where optimal convergence rates were obtained. The spectral approximation of elliptic operators by the HDG method was analyzed in [34], leading to a convergence of order h^{2k+1} for the eigenvalues; therein, a non-trivial post-processing using a Rayleigh quotient was also examined numerically leading to an improved convergence of order h^{2k+2} for $k \geq 1$. In contrast, the HHO approximation directly delivers a provable convergence of order h^{2k+2} even for $k = 0$. Finally, let us mention the recent work in [13, 20, 42] which studies numerically the optimally blended quadrature rules [2, 21] for the isogeometric analysis [36] of the Laplace eigenvalue problem and reports superconvergence of order h^{2k+2} for the eigenvalue errors while maintaining optimal convergence of orders h^k and h^{k+1} for the eigenfunction errors in the H^1-seminorm and in the L^2-norm, respectively.

The rest of this paper is organized as follows. Section 2 presents the second-order elliptic eigenvalue problem and briefly recalls the main abstract results we are going to use concerning the spectral approximation of compact operators in Hilbert spaces. Section 3 deals with the HHO discretization, first of the source problem and then of the eigenvalue problem. The algebraic realization of both problems is also presented. Section 3 additionally identifies the relevant notion of discrete solution operator for HHO methods and outlines the error analysis for the HHO discretization of the source problem. This analysis is based on the results of [28], but we handle the case where the exact solution does not have full regularity. Section 4 is concerned with the error analysis for the HHO discretization of the eigenvalue problem and contains our main results. Section 5 presents our numerical examples. Finally, some concluding remarks are collected in Section 6.

2. Functional setting

In this section, we present the second-order elliptic eigenvalue problem, and briefly recall the main abstract results on the approximation of the spectrum of compact operators in Hilbert spaces.

2.1. **Problem statement.** We consider the following second-order elliptic eigenvalue problem: find an eigenpair (λ, u) with $\lambda \in \mathbb{R}_{>0}$ and $u : \Omega \to \mathbb{R}$ such that

$$
\begin{aligned}
-\Delta u &= \lambda u \quad \text{in } \Omega, \\
u &= 0 \quad\ \text{on } \partial\Omega,
\end{aligned}
\tag{2.1}
$$

where $\Omega \subset \mathbb{R}^d$, $d \in \{1, 2, 3\}$, is a bounded open domain with Lipschitz boundary $\partial\Omega$ and Δ is the Laplacian. In weak form, the problem (2.1) reads as follows: find $(\lambda, u) \in \mathbb{R}_{>0} \times H_0^1(\Omega)$ such that

$$
a(u, w) = \lambda b(u, w) \qquad \forall w \in H_0^1(\Omega),
\tag{2.2}
$$

with the bilinear forms a and b defined on $H_0^1(\Omega) \times H_0^1(\Omega)$ and $L^2(\Omega) \times L^2(\Omega)$ as

$$
a(v, w) = (\nabla v, \nabla w)_{L^2(\Omega)}, \qquad b(v, w) = (v, w)_{L^2(\Omega)},
\tag{2.3}
$$

where $(\cdot, \cdot)_{L^2(\Omega)}$ denotes the inner product in $L^2(\Omega)$ or in $L^2(\Omega; \mathbb{R}^d)$. The eigenvalue problem (2.1) has a countably infinite sequence of eigenvalues $(\lambda_j)_{j \geq 1}$ (see, among many others, [12, Sec. 9.8]) such that

$$
0 < \lambda_1 < \lambda_2 \leq \lambda_3 \leq \cdots, \qquad \lambda_j \to +\infty,
\tag{2.4}
$$

and an associated sequence of L^2-orthonormal eigenfunctions $(u_j)_{j \geq 1}$ such that

$$
(u_j, u_l)_{L^2(\Omega)} = \delta_{jl} \qquad \forall j, l \geq 1,
\tag{2.5}
$$

with the Kronecker delta defined as $\delta_{jl} = 1$ when $j = l$ and zero otherwise.

The source problem associated with the eigenvalue problem (2.2) is as follows: for all $\phi \in L^2(\Omega)$, find $u \in H_0^1(\Omega)$ such that

$$
a(u, w) = b(\phi, w) \qquad \forall w \in H_0^1(\Omega).
\tag{2.6}
$$

The solution operator associated with (2.6) is denoted as $T : L^2(\Omega) \to L^2(\Omega)$, so that we have $T(\phi) \in H_0^1(\Omega) \subset L^2(\Omega)$ and

$$
a(T(\phi), w) = b(\phi, w) \qquad \forall w \in H_0^1(\Omega).
\tag{2.7}
$$

By the Rellich–Kondrachov Theorem (see, e.g., [35, Thm. 1.4.3.2]), T is compact from $L^2(\Omega)$ to $L^2(\Omega)$. Moreover, the elliptic regularity theory (see, e.g., [35, 37, 43]) implies that there is a real number $s \in (\frac{1}{2}, 1]$ so that $T \in \mathcal{L}(L^2(\Omega); H^{1+s}(\Omega))$. The reason for introducing the solution operator T is that $(\lambda, u) \in \mathbb{R}_{>0} \times H_0^1(\Omega)$ is an eigenpair for (2.2) if and only if $(\mu, u) \in \mathbb{R}_{>0} \times H_0^1(\Omega)$ with $\mu = \lambda^{-1}$ is an eigenpair of T.

One can also consider the adjoint solution operator $T^* : L^2(\Omega) \to L^2(\Omega)$ such that, for all $\psi \in L^2(\Omega)$, $T^*(\psi) \in H_0^1(\Omega)$ and

$$
a(w, T^*(\psi)) = b(w, \psi) \qquad \forall w \in H_0^1(\Omega).
\tag{2.8}
$$

The symmetry of the bilinear forms a and b implies that $T = T^*$; however, allowing more generality, we keep a distinct notation for the two operators. Since in general we have

$$
(T(\phi), \psi)_{L^2(\Omega)} = a(T(\phi), T^*(\psi)) = (\phi, T^*(\psi))_{L^2(\Omega)},
\tag{2.9}
$$

we infer that T^* is the adjoint operator of T, once the duality product is identified with the inner product in $L^2(\Omega)$. Therefore, in the present symmetric context, the operator T is selfadjoint.

2.2. **Spectral approximation theory for compact operators.** Let us now briefly recall the main results we use concerning the spectral approximation of compact operators in Hilbert spaces. Let L be a Hilbert space with inner product denoted by $(\cdot, \cdot)_L$, and let $T \in \mathcal{L}(L; L)$; assume that T is compact. We do not assume for the abstract theory that T is selfadjoint and we let $T^* \in \mathcal{L}(L; L)$ denote the adjoint operator of T. Let $T_n \in \mathcal{L}(L; L)$ be a member of a sequence of compact operators that converges to T in operator norm, i.e.,

$$(2.10) \qquad \lim_{n \to +\infty} \|T - T_n\|_{\mathcal{L}(L;L)} = 0,$$

and let $T_n^* \in \mathcal{L}(L; L)$ be the adjoint operator of T_n. We want to study how well the eigenvalues and the eigenfunctions of T_n approximate those of T. Let $\sigma(T)$ denote the spectrum of the operator T and let $\mu \in \sigma(T) \setminus \{0\}$ be a nonzero eigenvalue of T. Let α be the ascent of μ, i.e., the smallest integer α such that $\ker(\mu I - T)^\alpha = \ker(\mu I - T)^{\alpha+1}$, where I is the identity operator. Let also

$$(2.11) \qquad G_\mu = \ker(\mu I - T)^\alpha, \qquad G_\mu^* = \ker(\mu I - T^*)^\alpha,$$

and $m = \dim(G_\mu)$ (this integer is called the algebraic multiplicity of μ; note that $m \geq \alpha$).

Theorem 2.1 (Convergence of the eigenvalues). *Let $\mu \in \sigma(T) \setminus \{0\}$. Let α be the ascent of μ and let m be its algebraic multiplicity. Then there are m eigenvalues of T_n, denoted as $\mu_{n,1}, \ldots, \mu_{n,m}$, that converge to μ as $n \to +\infty$. Moreover, letting $\langle \mu_n \rangle = \frac{1}{m} \sum_{j=1}^m \mu_{n,j}$ denote their arithmetic mean, there is C, depending on μ but independent of n, such that*

$$(2.12) \qquad \max_{1 \leq j \leq m} |\mu - \mu_{n,j}|^\alpha + |\mu - \langle \mu_n \rangle| \leq C \Big(\sup_{\substack{0 \neq \phi \in G_\mu \\ 0 \neq \psi \in G_\mu^*}} \frac{|((T - T_n)\phi, \psi)_L|}{\|\phi\|_L \|\psi\|_L}$$
$$+ \|(T - T_n)|_{G_\mu}\|_{\mathcal{L}(G_\mu; L)} \|(T - T_n)^*|_{G_\mu^*}\|_{\mathcal{L}(G_\mu^*; L)} \Big).$$

Remark 2.2 (Convergence of the arithmetic mean). Note that (2.12) shows that for $\alpha \geq 2$, the arithmetic mean of the eigenvalues has a better convergence rate than each eigenvalue individually.

Theorem 2.3 (Convergence of the eigenfunctions). *Let $\mu \in \sigma(T) \setminus \{0\}$ with ascent α and algebraic multiplicity m. Let $\mu_{n,j}$ be an eigenvalue of T_n that converges to μ. Let $w_{n,j}$ be a unit vector in $\ker(\mu_{n,j} I - T_n)^\ell$ for some positive integer $\ell \leq \alpha$. Then, for any integer r with $\ell \leq r \leq \alpha$, there is a vector $u_r \in \ker(\mu I - T)^r \subset G_\mu$ such that*

$$(2.13) \qquad \|u_r - w_{n,j}\|_L \leq C \|(T - T_n)|_{G_\mu}\|_{\mathcal{L}(G_\mu; L)}^{\frac{r-\ell+1}{\alpha}},$$

where C depends on μ but is independent of n.

3. HHO DISCRETIZATION

In this section we present the discrete setting underlying the HHO discretization and then we describe the discretization of the source problem (2.6) and of the eigenvalue problem (2.2) by the HHO method. The HHO discretization of the source problem has been introduced and analyzed in [28]; herein, we complete the error analysis by addressing the case where the solution has minimal elliptic

regularity pickup. The devising and analysis of the HHO discretization of the eigenvalue problem is the main subject of this work.

3.1. **Discrete setting.** Let $\mathcal{K}$ be a partition of Ω into non-overlapping mesh cells. A generic mesh cell is denoted by K and can be a d-dimensional polytope with planar faces. In what follows, we assume that Ω is also a polytope in $\mathbb{R}^d$ with planar faces, so that the mesh can cover Ω exactly. For all $K \in \mathcal{K}$, we let $\boldsymbol{n}_K$ denote the unit outward vector to K. We say that $F \subset \mathbb{R}^d$ is a mesh face if it is a subset with non-empty relative interior of some affine hyperplane H_F and if one of the two following conditions holds true: either there are two distinct mesh cells $K_1, K_2 \in \mathcal{K}$ so that $F = \partial K_1 \cap \partial K_2 \cap H_F$ and F is called an interface, or there is one mesh cell $K \in \mathcal{K}$ so that $F = \partial K \cap \partial \Omega \cap H_F$ and F is called a boundary face. The mesh faces are collected in the set $\mathcal{F}$, interfaces in the set $\mathcal{F}^{\mathrm{i}}$, and boundary faces in the set $\mathcal{F}^{\mathrm{b}}$. We let h_S denote the diameter of the set S which can be a mesh cell or a mesh face. We assume that the mesh $\mathcal{K}$ is a member of a shape-regular polytopal mesh family in the sense specified in [27, 28]. In a nutshell, there is a matching simplicial submesh of $\mathcal{K}$ that belongs to a shape-regular family of simplicial meshes in the usual sense of Ciarlet [15] and such that each cell $K \in \mathcal{K}$ (resp., face $F \in \mathcal{F}$) can be decomposed in a finite number of subcells (resp., subfaces) with uniformly comparable diameter.

The HHO method is defined locally in each mesh cell $K \in \mathcal{K}$ from a pair of local unknowns which consist of one polynomial attached to the cell K and a piecewise polynomial attached to the boundary ∂K, i.e., one polynomial attached to each face F composing the boundary of K. Let $k \geq 0$ be a polynomial degree, and let $\mathbb{P}_{d'}^k(S)$, with $d' \in \{d-1, d\}$, be the linear space composed of real-valued polynomials of total degree at most k on the d'-dimensional affine manifold $S \subset \mathbb{R}^d$ (S is typically a mesh face or a mesh cell). The local discrete HHO pair is denoted

$$(3.1) \qquad \hat{v}_K = (v_K, v_{\partial K}) \in \hat{V}_K^k := \mathbb{P}_d^k(K) \times \mathbb{P}_{d-1}^k(\mathcal{F}_{\partial K}),$$

where

$$(3.2) \qquad \mathbb{P}_{d-1}^k(\mathcal{F}_{\partial K}) = \bigtimes_{F \in \mathcal{F}_{\partial K}} \mathbb{P}_{d-1}^k(F),$$

and $\mathcal{F}_{\partial K}$ is the collection of all the faces composing the cell boundary ∂K. There is actually some flexibility in the choice of the polynomial degree for the cell unknowns since one can take them to be polynomials of degree $l \in \{k-1, k, k+1\}$ [17]. For simplicity, we only consider the case $l = k$; all what follows readily extends to the other choices for l. In what follows, we always use hat symbols to indicate discrete HHO pairs.

There are two key ingredients to devise locally the HHO method: a local reconstruction operator and a local stabilization operator. The local reconstruction operator is defined as $p_K^{k+1} : \hat{V}_K^k \to \mathbb{P}_d^{k+1}(K)$ such that for all $\hat{v}_K = (v_K, v_{\partial K}) \in \hat{V}_K^k$, we have

$$(3.3) \quad (\nabla p_K^{k+1}(\hat{v}_K), \nabla w)_{L^2(K)} = (\nabla v_K, \nabla w)_{L^2(K)} + (v_{\partial K} - v_K, \nabla w \cdot \boldsymbol{n}_K)_{L^2(\partial K)}$$

for all $w \in \mathbb{P}_d^{k+1}(K)$. The above Neumann problem uniquely defines $p_K^{k+1}(\hat{v}_K) \in \mathbb{P}_d^{k+1}(K)$ up to an additive constant which can be specified by additionally requiring that $(p_K^{k+1}(\hat{v}_K) - v_K, 1)_{L^2(K)} = 0$ (this choice is irrelevant in what follows).

Concerning stabilization, we define the local operator $S_{\partial K}^k : \hat{V}_K^k \to \mathbb{P}_{d-1}^k(\mathcal{F}_{\partial K})$ such that, for all $\hat{v}_K = (v_K, v_{\partial K}) \in \hat{V}_K^k$, we have

$$(3.4) \qquad S_{\partial K}^k(\hat{v}_K) = \Pi_{\partial K}^k(v_{\partial K} - p_K^{k+1}(\hat{v}_K)_{|\partial K}) - \Pi_K^k(v_K - p_K^{k+1}(\hat{v}_K))_{|\partial K},$$

where Π_K^k and $\Pi_{\partial K}^k$ denote the L^2-orthogonal projectors from $L^1(K)$ onto $\mathbb{P}_d^k(K)$ and from $L^1(\partial K)$ onto $\mathbb{P}_{d-1}^k(\mathcal{F}_{\partial K})$, respectively. Equivalently, we have $S_{\partial K}^k(\hat{v}_K) = \Pi_{\partial K}^k(v_{\partial K} - P_K^{k+1}(\hat{v}_K)_{|\partial K})$ with $P_K^{k+1}(\hat{v}_K) = v_K + (I - \Pi_K^k)(p_K^{k+1}(\hat{v}_K))$, which is [28, eq. (22)]. Finally, the local HHO bilinear form for the stiffness is such that, for all $\hat{v}_K = (v_K, v_{\partial K}) \in \hat{V}_K^k$ and all $\hat{w}_K = (w_K, w_{\partial K}) \in \hat{V}_K^k$, we have
$$(3.5)$$
$$\hat{a}_K(\hat{v}_K, \hat{w}_K) = (\nabla p_K^{k+1}(\hat{v}_K), \nabla p_K^{k+1}(\hat{w}_K))_{L^2(K)} + (\tau_{\partial K} S_{\partial K}^k(\hat{v}_K), S_{\partial K}^k(\hat{w}_K))_{L^2(\partial K)},$$

where $\tau_{\partial K}$ denotes the piecewise constant function on ∂K such that $\tau_{\partial K|F} = \eta h_F^{-1}$ for all $F \in \mathcal{F}_{\partial K}$, and $\eta > 0$ is a user-specified positive stabilization parameter (the simplest choice is to set $\eta = 1$).

3.2. **HHO discretization of the source problem.** To discretize the source problem (2.6) using the HHO method, we consider the following global space of discrete HHO pairs:

$$(3.6) \qquad \hat{V}_h^k = V_{\mathcal{K}}^k \times V_{\mathcal{F}}^k, \qquad V_{\mathcal{K}}^k = \underset{K \in \mathcal{K}}{\times} \mathbb{P}_d^k(K), \qquad V_{\mathcal{F}}^k = \underset{F \in \mathcal{F}}{\times} \mathbb{P}_{d-1}^k(F).$$

Here, the subscript h refers to the global mesh-size defined as $h = \max_{K \in \mathcal{K}} h_K$. For a global HHO pair $\hat{v}_h = (v_{\mathcal{K}}, v_{\mathcal{F}}) \in \hat{V}_h^k$ with $v_{\mathcal{K}} \in V_{\mathcal{K}}^k$ and $v_{\mathcal{F}} \in V_{\mathcal{F}}^k$, we denote by $\hat{v}_K = (v_K, v_{\partial K}) \in \hat{V}_K^k$ the local HHO pair associated with the mesh cell $K \in \mathcal{K}$, and we denote by $v_F \in \mathbb{P}_{d-1}^k(F)$ the component associated with the mesh face $F \in \mathcal{F}$. The homogeneous Dirichlet boundary condition can be embedded into the HHO space by considering the subspaces

$$(3.7) \qquad \hat{V}_{h,0}^k := V_{\mathcal{K}}^k \times V_{\mathcal{F},0}^k, \qquad V_{\mathcal{F},0}^k := \{v_{\mathcal{F}} \in V_{\mathcal{F}}^k \mid v_F = 0 \quad \forall F \in \mathcal{F}^b\}.$$

The HHO discretization of the source problem with $\phi \in L^2(\Omega)$ reads as follows: find $\hat{u}_h \in \hat{V}_{h,0}^k$ such that

$$(3.8) \qquad \hat{a}_h(\hat{u}_h, \hat{w}_h) = b(\phi, w_{\mathcal{K}}) \qquad \forall \hat{w}_h = (w_{\mathcal{K}}, w_{\mathcal{F}}) \in \hat{V}_{h,0}^k,$$

where

$$(3.9) \qquad \hat{a}_h(\hat{v}_h, \hat{w}_h) = \sum_{K \in \mathcal{K}} \hat{a}_K(\hat{v}_K, \hat{w}_K) \qquad \forall \hat{v}_h, \hat{w}_h \in \hat{V}_h.$$

The algebraic realization of the discrete source problem (3.8) leads to a symmetric linear system which can be written in the following block form where unknowns attached to the mesh cells are ordered before unknowns attached to the mesh faces:

$$(3.10) \qquad \begin{bmatrix} \mathbf{A}_{\mathcal{K}\mathcal{K}} & \mathbf{A}_{\mathcal{K}\mathcal{F}} \\ \mathbf{A}_{\mathcal{F}\mathcal{K}} & \mathbf{A}_{\mathcal{F}\mathcal{F}} \end{bmatrix} \begin{bmatrix} \mathbf{U}_{\mathcal{K}} \\ \mathbf{U}_{\mathcal{F}} \end{bmatrix} = \begin{bmatrix} \phi_{\mathcal{K}} \\ \mathbf{0} \end{bmatrix}.$$

The system matrix is positive-definite owing to the coercivity of the bilinear form $\hat{a}_h$; see (3.25) below. A computationally-effective way to solve the above linear system is to use a Schur complement technique, also known as static condensation, where the cell unknowns are eliminated by expressing them locally in terms of the

face unknowns. This elimination is simple since the block-matrix $\mathbf{A}_{\mathcal{K}\mathcal{K}}$ is block-diagonal. The resulting linear system in terms of the face unknowns is

$$(3.11) \qquad \mathbf{K}_{\mathcal{F}\mathcal{F}}\mathbf{U}_{\mathcal{F}} = -\mathbf{A}_{\mathcal{F}\mathcal{K}}\mathbf{A}_{\mathcal{K}\mathcal{K}}^{-1}\boldsymbol{\phi}_{\mathcal{K}},$$

with the Schur complement matrix $\mathbf{K}_{\mathcal{F}\mathcal{F}} = \mathbf{A}_{\mathcal{F}\mathcal{F}} - \mathbf{A}_{\mathcal{F}\mathcal{K}}\mathbf{A}_{\mathcal{K}\mathcal{K}}^{-1}\mathbf{A}_{\mathcal{K}\mathcal{F}}$. As shown in [17], the linear system (3.11) is a global transmission problem (in which a given mesh face is locally coupled to the other mesh faces with which it shares a mesh cell) that expresses the equilibration of a suitable flux across all the mesh interfaces.

3.3. **HHO discretization of the eigenvalue problem.** The HHO discretization of the eigenvalue problem (2.2) consists of finding the discrete eigenpairs $(\lambda_h, \hat{u}_h) \in \mathbb{R}_{>0} \times \hat{V}_{h,0}^k$ such that

$$(3.12) \qquad \hat{a}_h(\hat{u}_h, \hat{w}_h) = \lambda_h b(u_{\mathcal{K}}, w_{\mathcal{K}}) \qquad \forall \hat{w}_h = (w_{\mathcal{K}}, w_{\mathcal{F}}) \in \hat{V}_{h,0}^k.$$

One key idea here is that the mass bilinear form on the right-hand side of (3.12) only involves discrete cell unknowns.

The algebraic realization of (3.12) is the matrix eigenvalue problem

$$(3.13) \qquad \begin{bmatrix} \mathbf{A}_{\mathcal{K}\mathcal{K}} & \mathbf{A}_{\mathcal{K}\mathcal{F}} \\ \mathbf{A}_{\mathcal{F}\mathcal{K}} & \mathbf{A}_{\mathcal{F}\mathcal{F}} \end{bmatrix} \begin{bmatrix} \mathbf{U}_{\mathcal{K}} \\ \mathbf{U}_{\mathcal{F}} \end{bmatrix} = \lambda_h \begin{bmatrix} \mathbf{B}_{\mathcal{K}\mathcal{K}} & \mathbf{0} \\ \mathbf{0} & \mathbf{0} \end{bmatrix} \begin{bmatrix} \mathbf{U}_{\mathcal{K}} \\ \mathbf{U}_{\mathcal{F}} \end{bmatrix}.$$

Since the face unknowns do not carry any mass, they can be eliminated, leading to the following matrix eigenvalue problem solely in terms of the cell unknowns:

$$(3.14) \qquad \mathbf{K}_{\mathcal{K}\mathcal{K}}\mathbf{U}_{\mathcal{K}} = \lambda_h \mathbf{B}_{\mathcal{K}\mathcal{K}}\mathbf{U}_{\mathcal{K}},$$

with the Schur complement matrix $\mathbf{K}_{\mathcal{K}\mathcal{K}} = \mathbf{A}_{\mathcal{K}\mathcal{K}} - \mathbf{A}_{\mathcal{K}\mathcal{F}}\mathbf{A}_{\mathcal{F}\mathcal{F}}^{-1}\mathbf{A}_{\mathcal{F}\mathcal{K}}$. Therefore, there are as many discrete eigenpairs as there are cell unknowns, i.e., the dimension of the polynomial space $\mathbb{P}_d^k$ times the number of mesh cells.

3.4. **HHO solution operators.** We now introduce the key operators that play a central role in the analysis of the HHO approximation of the eigenvalue problem. To motivate the approach, we observe that for the source problem (3.8), one can consider the cell-face HHO solution operator $\hat{T}_h : L^2(\Omega) \to \hat{V}_{h,0}^k$ so that

$$(3.15) \qquad \hat{a}_h(\hat{T}_h(\phi), \hat{w}_h) = b(\phi, w_{\mathcal{K}}) \qquad \forall \hat{w}_h = (w_{\mathcal{K}}, w_{\mathcal{F}}) \in \hat{V}_{h,0}^k.$$

However, this operator is not convenient to analyze the approximation of the eigenvalue problem since it does not map to a subspace of $L^2(\Omega)$. The key idea is then to introduce a cell HHO solution operator $T_{\mathcal{K}} : L^2(\Omega) \to V_{\mathcal{K}}^k \subset L^2(\Omega)$ by mimicking the elimination of the face unknowns presented above at the algebraic level for the eigenvalue problem.

As a first step, we define the operator $Z_{\mathcal{F},0} : V_{\mathcal{K}}^k \to V_{\mathcal{F},0}^k$ so that, for all $v_{\mathcal{K}} \in V_{\mathcal{K}}^k$, $Z_{\mathcal{F},0}(v_{\mathcal{K}}) \in V_{\mathcal{F},0}^k$ is defined as the unique solution of

$$(3.16) \qquad \hat{a}_h((v_{\mathcal{K}}, Z_{\mathcal{F},0}(v_{\mathcal{K}})), (0, w_{\mathcal{F}})) = 0 \qquad \forall w_{\mathcal{F}} \in V_{\mathcal{F},0}^k.$$

To allow for some generality, we also define the operator $Z_{\mathcal{F},0}^{\dagger} : V_{\mathcal{K}}^k \to V_{\mathcal{F},0}^k$ so that

$$(3.17) \qquad \hat{a}_h((0, w_{\mathcal{F}}), (v_{\mathcal{K}}, Z_{\mathcal{F},0}^{\dagger}(v_{\mathcal{K}}))) = 0 \qquad \forall w_{\mathcal{F}} \in V_{\mathcal{F},0}^k.$$

In the present setting where the bilinear form $\hat{a}_h$ is symmetric, the two operators $Z_{\mathcal{F},0}$ and $Z_{\mathcal{F},0}^{\dagger}$ coincide. As a second step, we define the bilinear form $a_{\mathcal{K}}$ on $V_{\mathcal{K}}^k \times V_{\mathcal{K}}^k$ such that

$$(3.18) \qquad a_{\mathcal{K}}(v_{\mathcal{K}}, w_{\mathcal{K}}) = \hat{a}_h((v_{\mathcal{K}}, Z_{\mathcal{F},0}(v_{\mathcal{K}})), (w_{\mathcal{K}}, Z_{\mathcal{F},0}^{\dagger}(w_{\mathcal{K}}))),$$

and introduce the solution operator $T_{\mathcal{K}} : L^2(\Omega) \to V_{\mathcal{K}}^k$ so that

$$(3.19) \qquad a_{\mathcal{K}}(T_{\mathcal{K}}(\phi), w_{\mathcal{K}}) = b(\phi, w_K) \qquad \forall w_{\mathcal{K}} \in V_{\mathcal{K}}^k.$$

Lemma 3.1 (HHO solution operator). *The following holds true:*

$$(3.20) \qquad \hat{T}_h(\phi) = (T_{\mathcal{K}}(\phi), (Z_{\mathcal{F},0} \circ T_{\mathcal{K}})(\phi)) \qquad \forall \phi \in L^2(\Omega).$$

Proof. Let $\phi \in L^2(\Omega)$. Let us set $u_{\mathcal{K}} = T_{\mathcal{K}}(\phi)$ so that $u_{\mathcal{K}} \in V_{\mathcal{K}}^k$ and $a_{\mathcal{K}}(u_{\mathcal{K}}, w_{\mathcal{K}}) = b(\phi, w_{\mathcal{K}})$ for all $w_{\mathcal{K}} \in V_{\mathcal{K}}^k$, and set $u_{\mathcal{F}} = (Z_{\mathcal{F},0} \circ T_{\mathcal{K}})(\phi) = Z_{\mathcal{F},0}(u_{\mathcal{K}})$ so that $u_{\mathcal{F}} \in V_{\mathcal{F},0}^k$. Setting $\hat{u}_h = (u_{\mathcal{K}}, u_{\mathcal{F}}) \in \hat{V}_{h,0}^k$, we need to verify that $\hat{u}_h$ solves the discrete HHO source problem, i.e.,

$$\hat{a}_h(\hat{u}_h, \hat{w}_h) = b(\phi, w_{\mathcal{K}}) \qquad \forall \hat{w}_h = (w_{\mathcal{K}}, w_{\mathcal{F}}) \in \hat{V}_{h,0}^k.$$

Considering first a test function in the form $\hat{w}_h = (w_{\mathcal{K}}, 0)$, we obtain

$$\hat{a}_h(\hat{u}_h, (w_{\mathcal{K}}, 0)) = \hat{a}_h((u_{\mathcal{K}}, Z_{\mathcal{F},0}(u_{\mathcal{K}})), (w_{\mathcal{K}}, 0))$$
$$= \hat{a}_h((u_{\mathcal{K}}, Z_{\mathcal{F},0}(u_{\mathcal{K}})), (w_{\mathcal{K}}, 0)) + \underbrace{\hat{a}_h((u_{\mathcal{K}}, Z_{\mathcal{F},0}(u_{\mathcal{K}})), (0, Z_{\mathcal{F},0}^{\dagger}(w_{\mathcal{K}})))}_{=0}$$
$$= \hat{a}_h((u_{\mathcal{K}}, Z_{\mathcal{F},0}(u_{\mathcal{K}})), (w_{\mathcal{K}}, Z_{\mathcal{F},0}^{\dagger}(w_{\mathcal{K}})))$$
$$= a_{\mathcal{K}}(u_{\mathcal{K}}, w_{\mathcal{K}}) = b(\phi, w_{\mathcal{K}}),$$

where we used the definition (3.16) of $Z_{\mathcal{F},0}$ in the second line and the definition (3.18) of $a_{\mathcal{K}}$ in the fourth line. Considering now a test function in the form $\hat{w}_h = (0, w_{\mathcal{F}})$, we obtain owing to (3.16) that

$$\hat{a}_h(\hat{u}_h, (0, w_{\mathcal{F}})) = \hat{a}_h((u_{\mathcal{K}}, Z_{\mathcal{F},0}(u_{\mathcal{K}})), (0, w_{\mathcal{F}})) = 0.$$

This completes the proof. $\qquad\square$

The cell HHO solution operator $T_{\mathcal{K}}$ defined in (3.19) is the relevant solution operator for the discrete eigenvalue problem (3.12). Indeed, the eigenpair $(\lambda_h, \hat{u}_h) \in \mathbb{R}_{>0} \times \hat{V}_{h,0}^k$ with $\hat{u}_h = (u_{\mathcal{K}}, u_{\mathcal{F}}) \in V_{\mathcal{K}}^k \times V_{\mathcal{F},0}^k$ solves (3.12) if and only if $u_{\mathcal{F}} = Z_{\mathcal{F},0}(u_{\mathcal{K}})$ and the pair $(\lambda_h, u_{\mathcal{K}}) \in \mathbb{R}_{>0} \times V_{\mathcal{K}}^k$ solves

$$(3.21) \qquad a_{\mathcal{K}}(u_{\mathcal{K}}, w_{\mathcal{K}}) = \lambda_h b(u_{\mathcal{K}}, w_{\mathcal{K}}) \qquad \forall w_{\mathcal{K}} \in V_{\mathcal{K}}^k,$$

that is, if and only if $(\mu_h, u_{\mathcal{K}}) \in \mathbb{R}_{>0} \times V_{\mathcal{K}}^k$ with $\mu_h = \lambda_h^{-1}$ is an eigenpair of the discrete solution operator $T_{\mathcal{K}}$.

3.5. **Error analysis for the source problem.** In this section we briefly outline the analysis of the HHO discretization of the source problem drawing on the ideas introduced in [28]. One difference here is to include the case when the exact solution has a smoothness index $s \in (\frac{1}{2}, k+2]$ and not just $s = k+2$ (recall that $s > \frac{1}{2}$ follows from the elliptic regularity theory). In what follows, we use the symbol C to denote a generic constant (its value can change at each occurrence) that can depend on the mesh regularity, the polynomial degree k, and the domain Ω, but is independent of the mesh-size h.

Let $K \in \mathcal{K}$ be a mesh cell. We equip the local HHO space $\hat{V}_K^k$ defined in (3.1) with the following seminorm (which is an HHO counterpart of the $H^1(K)$-seminorm):

$$(3.22) \qquad \|\hat{v}_K\|_{\hat{V}_K^k}^2 = \|\nabla v_K\|_{L^2(K)}^2 + \|\tau_{\partial K}^{\frac{1}{2}}(v_K - v_{\partial K})\|_{L^2(\partial K)}^2$$

for all $\hat{v}_K = (v_K, v_{\partial K}) \in \hat{V}_K^k$. We observe that $\|\hat{v}_K\|_{\hat{V}_K^k} = 0$ implies that v_K and $v_{\partial K}$ are constant functions taking the same value. We equip the global HHO space $\hat{V}_h^k$ defined in (3.6) with the seminorm (which is an HHO counterpart of the $H^1(\Omega)$-seminorm)

$$(3.23) \qquad \|\hat{v}_h\|_{\hat{V}_h^k}^2 = \sum_{K \in \mathcal{K}} \|\hat{v}_K\|_{\hat{V}_K^k}^2 \qquad \forall \hat{v}_h \in \hat{V}_h^k.$$

The map $\|\cdot\|_{\hat{V}_h^k}$ is a norm on the subspace $\hat{V}_{h,0}^k$ defined in (3.7). [28, Lemma 4] shows that there is a real number $\beta > 0$, uniform with respect to the mesh-size h, such that, for all $K \in \mathcal{K}$,

$$(3.24) \qquad \beta\|\hat{v}_K\|_{\hat{V}_K^k}^2 \le \hat{a}_K(\hat{v}_K, \hat{v}_K) \le \beta^{-1}\|\hat{v}_K\|_{\hat{V}_K^k}^2 \qquad \forall \hat{v}_K \in \hat{V}_K^k,$$

and, consequently, given the definition (3.9) of $\hat{a}_h$, that the following coercivity and boundedness properties hold true:

$$(3.25) \qquad \hat{a}_h(\hat{v}_h, \hat{v}_h) \ge \beta\|\hat{v}_h\|_{\hat{V}_h^k}^2 \qquad\qquad \forall \hat{v}_h \in \hat{V}_h^k,$$

$$(3.26) \qquad \hat{a}_h(\hat{v}_h, \hat{w}_h) \le \beta^{-1}\|\hat{v}_h\|_{\hat{V}_h^k}\|\hat{w}_h\|_{\hat{V}_h^k} \qquad \forall(\hat{v}_h, \hat{w}_h) \in \hat{V}_h^k \times \hat{V}_h^k.$$

Owing to the Lax–Milgram Lemma, we infer that the cell-face HHO solution operator $\hat{T}_h : L^2(\Omega) \to \hat{V}_{h,0}^k$ introduced in (3.15) is well-defined. For later use in the analysis of the eigenvalue problem, we now establish a stability property for $\hat{T}_h$.

Lemma 3.2 (Stability of $\hat{T}_h$). *There is C so that*

$$(3.27) \qquad \|\hat{T}_h(\phi)\|_{\hat{V}_h^k} \le C\|\phi\|_{L^2(\Omega)} \qquad \forall \phi \in L^2(\Omega).$$

Proof. Let $\phi \in L^2(\Omega)$ and let us write $\hat{T}_h(\phi) = (u_{\mathcal{K}}, u_{\mathcal{F}})$ with $u_{\mathcal{K}} \in V_{\mathcal{K}}^k$ and $u_{\mathcal{F}} \in V_{\mathcal{F},0}^k$. Using the coercivity property (3.25), the definition (3.15) of the solution operator $\hat{T}_h$, that of the bilinear form b, and the Cauchy–Schwarz inequality lead to

$$(3.28) \qquad \beta\|\hat{T}_h(\phi)\|_{\hat{V}_h^k}^2 \le \hat{a}_h(\hat{T}_h(\phi), \hat{T}_h(\phi)) = b(\phi, u_{\mathcal{K}}) \le \|\phi\|_{L^2(\Omega)}\|u_{\mathcal{K}}\|_{L^2(\Omega)}.$$

On the broken polynomial space $V_{\mathcal{K}}^k$, we can apply the following discrete Poincaré inequality which has been derived in the discontinuous Galerkin context in [4, 11, 26]:

$$C_{\mathrm{P,dG}}\|u_{\mathcal{K}}\|_{L^2(\Omega)} \le \left(\sum_{K \in \mathcal{K}} \|\nabla u_K\|_{L^2(K)}^2 + \sum_{F \in \mathcal{F}} h_F^{-1}\|[u_{\mathcal{K}}]_F\|_{L^2(F)}^2 \right)^{\frac{1}{2}},$$

with $C_{\mathrm{P,dG}} > 0$ uniform with respect to the mesh-size h, and where $[u_{\mathcal{K}}]_F$ denotes the jump of $u_{\mathcal{K}}$ across F if F is an interface ($F \in \mathcal{F}^{\mathrm{i}}$) or the value of $u_{\mathcal{K}}$ on F if F is a boundary face ($F \in \mathcal{F}^{\mathrm{b}}$). If $F \in \mathcal{F}^{\mathrm{i}}$, we have $[u_{\mathcal{K}}]_F = u_{K_1}|_F - u_{K_2}|_F$, where K_1, K_2 are the two mesh cells sharing F (the sign of the jump is irrelevant in what follows), and we can therefore write $[u_{\mathcal{K}}]_F = (u_{K_1} - u_F)|_F - (u_{K_2} - u_F)|_F$, where u_F is the component of $u_{\mathcal{F}}$ attached to F. If $F \in \mathcal{F}^{\mathrm{b}}$, we have $[u_{\mathcal{K}}]_F = u_{K_1}|_F$, where K_1 is the unique mesh cell sharing F with $\partial\Omega$, and we can therefore write $[u_{\mathcal{K}}]_F = (u_{K_1} - u_F)|_F$ since $u_F \equiv 0$ (recall that $u_{\mathcal{F}} \in V_{\mathcal{F},0}^k$). Recalling the definition (3.23) of the $\|\cdot\|_{\hat{V}_h^k}$-norm, that of $\tau_{\partial K}$ given just below (3.5), and using the triangle inequality, we infer that

$$\|u_{\mathcal{K}}\|_{L^2(\Omega)} \le C\|(u_{\mathcal{K}}, u_{\mathcal{F}})\|_{\hat{V}_h^k} = C\|\hat{T}_h(\phi)\|_{\hat{V}_h^k}.$$

Combining this bound with (3.28), we obtain the assertion. $\qquad\square$

An important tool in the analysis of HHO methods is the global reduction operator $\hat{I}_h^k : H_0^1(\Omega) \to \hat{V}_{h,0}^k$ defined such that, for all $v \in H_0^1(\Omega)$,

$$(3.29) \qquad \hat{I}_h^k(v) = (\Pi_\mathcal{K}^k(v), \Pi_\mathcal{F}^k(v)) := ((\Pi_K^k(v))_{K\in\mathcal{K}}, (\Pi_F^k(v))_{F\in\mathcal{F}}) \in \hat{V}_{h,0}^k,$$

where Π_K^k and Π_F^k denote the L^2-orthogonal projectors onto $\mathbb{P}_d^k(K)$ and $\mathbb{P}_{d-1}^k(F)$, respectively. We also define the local reduction operator $\hat{I}_K^k : H^1(K) \to \hat{V}_K^k$ such that, for all $v \in H^1(K)$,

$$(3.30) \qquad \hat{I}_K^k(v) = (\Pi_K^k(v), \Pi_{\partial K}^k(v)) = (\Pi_K^k(v), (\Pi_F^k(v))_{F\in\mathcal{F}_{\partial K}}) \in \hat{V}_K^k.$$

Recalling the local reconstruction operator $p_K^{k+1} : \hat{V}_K^k \to \mathbb{P}_d^{k+1}(K)$ defined in (3.3), [28, Lemma 3] shows that

$$(3.31) \qquad e_K^{k+1} := p_K^{k+1} \circ \hat{I}_K^k : H^1(K) \to \mathbb{P}_d^{k+1}(K)$$

is the elliptic projector, i.e., for all $v \in H^1(K)$, $e_K^{k+1}(v)$ is the unique polynomial in $\mathbb{P}_d^{k+1}(K)$ such that $(\nabla(e_K^{k+1}(v) - v), \nabla w)_{L^2(K)} = 0$ for all $w \in \mathbb{P}_d^{k+1}(K)$ and $(e_K^{k+1}(v) - v, 1)_{L^2(K)} = 0$. For two functions $v, w \in H^1(K)$, the above orthogonality condition on the gradient implies that

$$(3.32) \qquad \begin{aligned} &(\nabla(e_K^{k+1}(v) - v), \nabla(e_K^{k+1}(w) - w))_{L^2(K)} \\ &= (\nabla v, \nabla w)_{L^2(K)} - (\nabla e_K^{k+1}(v), \nabla e_K^{k+1}(w))_{L^2(K)}. \end{aligned}$$

Lemma 3.3 (Discrete error estimate). *There is C such that*

$$(3.33) \qquad \|\hat{T}_h(\phi) - \hat{I}_h^k(T(\phi))\|_{\hat{V}_h^k} \le Ch^t \|T(\phi)\|_{H^{1+t}(\Omega)}$$

for all $t \in [s, k+1]$ and all $\phi \in L^2(\Omega)$ such that $T(\phi) \in H^{1+t}(\Omega)$; here, $s > \frac{1}{2}$ is the smoothness index resulting from the elliptic regularity theory.

Proof. Let $t \in [s, k+1]$, and let $\phi \in L^2(\Omega)$ be such that $T(\phi) \in H^{1+t}(\Omega)$. Proceeding as in the proof of [28, Theorem 8], we infer that

$$\|\hat{T}_h(\phi) - \hat{I}_h^k(T(\phi))\|_{\hat{V}_h^k} \le C \sup_{\substack{\hat{w}_h \in \hat{V}_{h,0}^k \\ \|\hat{w}_h\|_{\hat{V}_h^k}=1}} |\delta_h(\hat{w}_h)| =: C \|\delta_h\|_{(\hat{V}_{h,0}^k)'},$$

with the consistency error $\delta_h(\hat{w}_h)$ such that

$$\begin{aligned} \delta_h(\hat{w}_h) = &\sum_{K\in\mathcal{K}} (\nabla\xi_K, \nabla w_K)_{L^2(K)} + (\nabla\xi_K \cdot \boldsymbol{n}_K, w_{\partial K} - w_K)_{L^2(\partial K)} \\ &+ (\tau_{\partial K} S_{\partial K}^k(\hat{I}_K^k(u)), S_{\partial K}^k(\hat{w}_K))_{L^2(\partial K)}, \end{aligned}$$

and the shorthand notation $\xi_K := e_K^{k+1}(u_{|K}) - u_{|K}$ and $u = T(\phi)$ (we used $s > \frac{1}{2}$ in writing the second summand on the right-hand side above). Using the Cauchy–Schwarz inequality and recalling the definition of the norm $\|\hat{w}_h\|_{\hat{V}_h^k}$, we obtain

$$\|\delta_h\|_{(\hat{V}_{h,0}^k)'} \le C \left(\sum_{K\in\mathcal{K}} \|\nabla\xi_K\|_{L^2(K)}^2 + h_K \|\nabla\xi_K\|_{L^2(\partial K)}^2 + h_K^{-1} \|S_{\partial K}^k(\hat{I}_K^k(u))\|_{L^2(\partial K)}^2 \right)^{\frac{1}{2}}.$$

Recalling the definition (3.4) of the stabilization operator $S_{\partial K}^k$, we obtain that

$$\begin{aligned}
S_{\partial K}^k(\hat{I}_K^k(u)) &= \Pi_{\partial K}^k(\Pi_{\partial K}^k(u) - e_K^{k+1}(u)_{|\partial K}) - \Pi_K^k(\Pi_{\partial K}^k(u) - e_K^{k+1}(u))_{|\partial K} \\
&= \Pi_{\partial K}^k((u - e_K^{k+1}(u))_{|\partial K}) - \Pi_K^k(u - e_K^{k+1}(u))_{|\partial K} \\
&= -\Pi_{\partial K}^k((\xi_K)_{|\partial K}) + \Pi_K^k(\xi_K)_{|\partial K}.
\end{aligned}$$

We then have

$$\begin{aligned}
\|S_{\partial K}^k(\hat{I}_K^k(u))\|_{L^2(\partial K)} &\leq \|\xi_K\|_{L^2(\partial K)} + \|\Pi_K^k(\xi_K)\|_{L^2(\partial K)} \\
&\leq \|\xi_K\|_{L^2(\partial K)} + Ch_K^{-\frac{1}{2}}\|\xi_K\|_{L^2(K)} \\
&\leq C(h_K^{-\frac{1}{2}}\|\xi_K\|_{L^2(K)} + h_K^{\frac{1}{2}}\|\nabla\xi_K\|_{L^2(K)}) \\
&\leq Ch_K^{\frac{1}{2}}\|\nabla\xi_K\|_{L^2(K)},
\end{aligned}$$

where we used a triangle inequality and the L^2-stability of $\Pi_{\partial K}^k$ in the first line, a discrete trace inequality and the L^2-stability of Π_K^k in the second line, a multiplicative trace inequality in the third line, and the Poincaré–Steklov inequality on K in the fourth line (that is, $\|\xi_K\|_{L^2(K)} \leq Ch_K\|\nabla\xi_K\|_{L^2(K)}$ since ξ_K has zero mean-value in K by construction). We conclude that $h_K^{-\frac{1}{2}}\|S_{\partial K}^k(\hat{I}_K^k(u))\|_{L^2(\partial K)} \leq C\|\nabla\xi_K\|_{L^2(K)}$ for some generic constant C, and, therefore, we have

$$\|\delta_h\|_{(\hat{V}_{h,0}^k)'} \leq C\left(\sum_{K \in \mathcal{K}} \|\nabla\xi_K\|_{L^2(K)}^2 + h_K\|\nabla\xi_K\|_{L^2(\partial K)}^2\right)^{\frac{1}{2}}.$$

Finally, invoking the approximation properties of the elliptic projector on all the mesh cells leads to the assertion. $\qquad\square$

4. Error analysis for the eigenvalue problem

The goal of this section is to perform the error analysis of the discrete eigenvalue problem (3.12) by using the abstract theory outlined in Section 2.2 in the Hilbert space $L = L^2(\Omega)$. Let $T, T^* : L^2(\Omega) \to H_0^1(\Omega) \subset L^2(\Omega)$ be the exact solution and adjoint solution operators defined in Section 2.1 ($T = T^*$, i.e., T is selfadjoint, in the present symmetric setting). Let $T_{\mathcal{K}} : L \to V_{\mathcal{K}}^k \subset L$ be the discrete HHO solution operator defined in (3.19). Its adjoint operator $T_{\mathcal{K}}^* : L \to V_{\mathcal{K}} \subset L$ is defined so that, for all $\psi \in L$, $T_{\mathcal{K}}^*(\psi) \in V_{\mathcal{K}}$ is the unique solution of

$$(4.1) \qquad a_{\mathcal{K}}(w_{\mathcal{K}}, T_{\mathcal{K}}^*(\psi)) = b(w_{\mathcal{K}}, \psi) \qquad \forall w_{\mathcal{K}} \in V_{\mathcal{K}}^k.$$

Owing to the symmetry of the bilinear forms $a_{\mathcal{K}}$ and b, we have $T_{\mathcal{K}} = T_{\mathcal{K}}^*$ in the present setting, i.e., $T_{\mathcal{K}}$ is selfadjoint. We keep as before a distinct notation to allow for more generality, and we also set $\hat{T}_h^{\dagger} : L \to \hat{V}_{h,0}^k$ so that $\hat{T}_h^{\dagger}(\psi) = (T_{\mathcal{K}}^*(\psi), (Z_{\mathcal{F},0}^{\dagger} \circ T_{\mathcal{K}}^*)(\psi))$ for all $\psi \in L$. Proceeding as in Lemma 3.1, we conclude that

$$(4.2) \qquad \hat{a}_h(\hat{w}_h, \hat{T}_h^{\dagger}(\psi)) = b(w_{\mathcal{K}}, \psi) \qquad \forall \hat{w}_h = (w_{\mathcal{K}}, w_{\mathcal{F}}) \in \hat{V}_{h,0}^k.$$

In the present symmetric setting, we have $\hat{T}_h = \hat{T}_h^{\dagger}$ with $\hat{T}_h$ defined in (3.15). Finally, the elliptic regularity theory implies that there is a real number $s \in (\frac{1}{2}, 1]$ so that $T, T^* \in \mathcal{L}(L^2(\Omega); H^{1+s}(\Omega))$, with operator norm denoted by C_s.

4.1. **Preliminary results.** To verify that we can apply the abstract theory from Section 2.2, let us show that $T_{\mathcal{K}}$ converges to T in operator norm as the mesh-size h tends to zero, i.e., that (2.10) holds true.

Lemma 4.1 (Bound on $L \times L$). *The following holds true:*

$$(4.3) \qquad \sup_{(\phi,\psi)\in L\times L} |((T-T_{\mathcal{K}})(\phi),\psi)_L| \le Ch^s\|\phi\|_L\|\psi\|_L,$$

where $s \in (\frac{1}{2}, 1]$ is the smoothness index associated with the elliptic regularity theory. Consequently, we have $\|T - T_{\mathcal{K}}\|_{\mathcal{L}(L;L)} \to 0$ as $h \to 0$.

Proof. For all $\phi, \psi \in L$, we have

$$((T-T_{\mathcal{K}})(\phi),\psi)_L$$
$$= (T(\phi),\psi)_L - b(T_{\mathcal{K}}(\phi),\psi)$$
$$= (T(\phi),\psi)_L - a_{\mathcal{K}}(T_{\mathcal{K}}(\phi),T_{\mathcal{K}}^*(\psi))$$
$$= (T(\phi),\psi)_L - \hat{a}_h(\hat{T}_h(\phi),\hat{T}_h^\dagger(\psi))$$
$$= (T(\phi),\psi)_L - \hat{a}_h(\hat{I}_h^k(T(\phi)),\hat{T}_h^\dagger(\psi)) + \hat{a}_h(\hat{I}_h^k(T(\phi)) - \hat{T}_h(\phi),\hat{T}_h^\dagger(\psi))$$
$$(4.4) \qquad = (T(\phi) - \Pi_{\mathcal{K}}^k(T(\phi)),\psi)_L + \hat{a}_h(\hat{I}_h^k(T(\phi)) - \hat{T}_h(\phi),\hat{T}_h^\dagger(\psi)),$$

where we used the definition of the bilinear form b in the first line, the definition (4.1) of $T_{\mathcal{K}}^*$ in the second line, the definition (3.18) of $a_{\mathcal{K}}$ and Lemma 3.1 in the third line, a simple algebraic manipulation in the fourth line, and the property (4.2) and the definition (3.29) of $\hat{I}_h^k$ in the fifth line. Let us call S_1, S_2 the two summands on the right-hand side of (4.4). Owing to the elliptic regularity theory and the approximation properties of the projector $\Pi_{\mathcal{K}}^k$ (with $k \ge 0$), we obtain that

$$|S_1| \le Ch|T(\phi)|_{H^1(\Omega)}\|\psi\|_L.$$

Since $|T(\phi)|_{H^1(\Omega)} \le \|T(\phi)\|_{H^{1+s}(\Omega)} \le C_s\|\phi\|_L$, we infer that

$$|S_1| \le CC_s h\|\phi\|_L\|\psi\|_L.$$

To bound S_2, we use the boundedness property (3.26) of $\hat{a}_h$ followed by the error estimate from Lemma 3.3 (with $t = s$) and the stability property of $\hat{T}_h^\dagger = \hat{T}_h$ from Lemma 3.2 to infer that

$$|S_2| \le Ch^s\|T(\phi)\|_{H^{1+s}(\Omega)}\|\psi\|_L \le CC_s h^s\|\phi\|_L\|\psi\|_L.$$

Combining the bounds on S_1 and S_2 concludes the proof. $\qquad \square$

Let $\mu \in \sigma(T) \setminus \{0\}$ with ascent α and algebraic multiplicity m. To quantify the smoothness of the functions in the subspaces G_μ and G_μ^* defined in (2.11), we assume that there is a real number $t \in [s, k+1]$ and a constant C_t so that

$$(4.5) \qquad \begin{aligned} \|\phi\|_{H^{1+t}(\Omega)} + \|T(\phi)\|_{H^{1+t}(\Omega)} &\le C_t\|\phi\|_L & \forall\phi \in G_\mu, \\ \|\psi\|_{H^{1+t}(\Omega)} + \|T^*(\psi)\|_{H^{1+t}(\Omega)} &\le C_t\|\psi\|_L & \forall\psi \in G_\mu^*. \end{aligned}$$

Note that t depends on μ, but we just write t instead of t_μ to alleviate the notation. If $t = s$, functions in G_μ and G_μ^* do not provide additional smoothness with respect to that resulting from the elliptic regularity theory. In general, functions in G_μ and G_μ^* are smoother, and one has $t > s$. The case $t = k+1$ leads to optimal error estimates; see Remark 4.7 below.

Lemma 4.2 (Bound on $G_\mu \times L$ and $L \times G_\mu^*$). *The following holds true:*

$$(4.6) \qquad \sup_{(\phi,\psi) \in G_\mu \times L} |((T - T_\mathcal{K})(\phi), \psi)_L| \leq Ch^t \|\phi\|_L \|\psi\|_L,$$

where $t \in [s, k+1]$ is the smoothness index associated with μ. Consequently, we have

$$(4.7) \qquad \|(T - T_\mathcal{K})|_{G_\mu}\|_{\mathcal{L}(G_\mu; L)} \leq Ch^t.$$

Similar bounds hold for $T_\mathcal{K}^*$, and, in particular, we have $\|(T - T_\mathcal{K})^*|_{G_\mu^*}\|_{\mathcal{L}(G_\mu^*; L)} \leq Ch^t$.

Proof. We only prove the statement for $T_\mathcal{K}$, the other proof is similar. Our starting point is (4.4). Owing to the smoothness of the function $T(\phi)$ resulting from (4.5), we infer that

$$|S_1| \leq Ch^{\min(k+1, t+1)} \|T(\phi)\|_{H^{1+t}(\Omega)} \|\psi\|_L \leq CC_t h^{\min(k+1, t+1)} \|\phi\|_L \|\psi\|_L.$$

Using similar arguments leads to $|S_2| \leq Ch^t \|\phi\|_L \|\psi\|_L$. Since $t \leq \min(k+1, t+1)$, the assertion follows. $\qquad\square$

Lemma 4.3 (Bound on $G_\mu \times G_\mu^*$). *The following holds true:*

$$(4.8) \qquad \sup_{(\phi,\psi) \in G_\mu \times G_\mu^*} |((T - T_\mathcal{K})(\phi), \psi)_L| \leq Ch^{2t} \|\phi\|_L \|\psi\|_L,$$

where $t \in [s, k+1]$ is the smoothness index associated with μ.

Proof. Our starting point is again (4.4), but we can now derive sharper bounds on the two summands S_1 and S_2 by exploiting the smoothness of both ϕ and ψ. On the one hand, we have

$$S_1 = (T(\phi) - \Pi_\mathcal{K}^k(T(\phi)), \psi)_L = (T(\phi) - \Pi_\mathcal{K}^k(T(\phi)), \psi - \Pi_\mathcal{K}^k(\psi))_L,$$

so that

$$|S_1| \leq Ch^{2\min(k+1, t+1)} \|T(\phi)\|_{H^{1+t}(\Omega)} \|\psi\|_{H^{1+t}(\Omega)} \leq CC_t^2 h^{2\min(k+1, t+1)} \|\phi\|_L \|\psi\|_L,$$

where we used the smoothness of the functions $T(\phi)$ and ψ resulting from (4.5). On the other hand, we have

$$\begin{aligned}
S_2 &= \hat{a}_h(\hat{I}_h^k(T(\phi)) - \hat{T}_h(\phi), \hat{T}_h^\dagger(\psi)) \\
&= \hat{a}_h(\hat{I}_h^k(T(\phi)) - \hat{T}_h(\phi), \hat{I}_h^k(T^*(\psi))) + \hat{a}_h(\hat{I}_h^k(T(\phi)) - \hat{T}_h(\phi), \hat{T}_h^\dagger(\psi) - \hat{I}_h^k(T^*(\psi))) \\
&= a(T(\phi), T^*(\psi)) - \hat{a}_h(\hat{T}_h(\phi), \hat{I}_h^k(T^*(\psi))) \\
&\quad + \hat{a}_h(\hat{I}_h^k(T(\phi)), \hat{I}_h^k(T^*(\psi))) - a(T(\phi), T^*(\psi)) \\
&\quad + \hat{a}_h(\hat{I}_h^k(T(\phi)) - \hat{T}_h(\phi), \hat{T}_h^\dagger(\psi) - \hat{I}_h^k(T^*(\psi))) \\
&= (\phi - \Pi_\mathcal{K}^k(\phi), T^*(\psi) - \Pi_\mathcal{K}^k(T^*(\psi)))_L \\
&\quad + \hat{a}_h(\hat{I}_h^k(T(\phi)), \hat{I}_h^k(T^*(\psi))) - a(T(\phi), T^*(\psi)) \\
&\quad + \hat{a}_h(\hat{I}_h^k(T(\phi)) - \hat{T}_h(\phi), \hat{T}_h^\dagger(\psi) - \hat{I}_h^k(T^*(\psi))),
\end{aligned}$$

where we used simple algebraic manipulations to derive the second and third identities, and the definition of T together with that of $\hat{T}_h$ and of $\hat{I}_h^k$ to derive the last identity. Let us call $S_{2,1}$, $S_{2,2}$, $S_{2,3}$ the three summands on the right-hand side

of the above equation. Reasoning as above and invoking the smoothness of the functions ϕ and $T^*(\psi)$ resulting from (4.5), we infer that

$$|S_{2,1}| \leq CC_t^2 h^{2\min(k+1,t+1)} \|\phi\|_L \|\psi\|_L.$$

To bound $S_{2,2}$, we observe that

$$
\begin{aligned}
S_{2,2} = &\sum_{K \in \mathcal{K}} (\nabla e_K^{k+1}(T(\phi)), \nabla e_K^{k+1}(T^*(\psi)))_{L^2(K)} - (\nabla T(\phi), \nabla T^*(\psi))_{L^2(K)} \\
&+ \sum_{K \in \mathcal{K}} (\tau_{\partial K} S_{\partial K}^k(\hat{I}_h^k(T(\phi))), S_{\partial K}^k(\hat{I}_h^k(T^*(\phi))))_{L^2(\partial K)} =: S_{2,2,1} + S_{2,2,2}.
\end{aligned}
$$

Since e_K^{k+1} is the elliptic projector, the identity (3.32) implies that

$$S_{2,2,1} = \sum_{K \in \mathcal{K}} -(\nabla(T(\phi) - e_K^{k+1}(T(\phi))), \nabla(T^*(\psi) - e_K^{k+1}(T^*(\psi))))_{L^2(K)}.$$

Using the Cauchy–Schwarz inequality and the approximation properties of the elliptic projector, we infer that

$$|S_{2,2,1}| \leq Ch^{2t}\|T(\phi)\|_{H^{1+t}(\Omega)}\|T^*(\psi)\|_{H^{1+t}(\Omega)} \leq CC_t^2 h^{2t}\|\phi\|_L \|\psi\|_L.$$

Moreover, reasoning as in the end of the proof of Lemma 3.3, we obtain that

$$|S_{2,2,2}| \leq Ch^{2t}\|T(\phi)\|_{H^{1+t}(\Omega)}\|T^*(\psi)\|_{H^{1+t}(\Omega)} \leq CC_t^2 h^{2t}\|\phi\|_L \|\psi\|_L.$$

Hence, we have

$$|S_{2,2}| \leq CC_t^2 h^{2t}\|\phi\|_L \|\psi\|_L.$$

Finally, the bound on $S_{2,3}$ results from the boundedness property (3.26) of $\hat{a}_h$ and the error estimate from Lemma 3.3 since

$$|S_{2,3}| \leq Ch^{2t}\|T(\phi)\|_{H^{1+t}(\Omega)}\|T^*(\psi)\|_{H^{1+t}(\Omega)} \leq CC_t^2 h^{2t}\|\phi\|_L \|\psi\|_L.$$

Collecting the above estimates concludes the proof. □

4.2. **Main results.** We can now present our main results. Let $\mu \in \sigma(T) \setminus \{0\}$ with ascent α and algebraic multiplicity m. We focus now on the spectral approximation of selfadjoint operators, so that we have $\alpha = 1$. Owing to the convergence result from Lemma 4.1, there are m eigenvalues of $T_\mathcal{K}$, denoted $\mu_{h,1}, \ldots, \mu_{h,m}$, that converge to μ as $h \to 0$.

Theorem 4.4 (Error estimate on eigenvalues and eigenfunctions in L). *Assume that there is $t \in [s, k+1]$ so that the smoothness property (4.5) holds true, where $s > \frac{1}{2}$ is the smoothness index resulting from the elliptic regularity theory. Then there is C, depending on μ (and on the mesh regularity, the polynomial degree k, and the domain Ω) but independent of the mesh-size h, such that*

$$(4.9) \qquad \max_{1 \leq j \leq m} |\mu - \mu_{h,j}| \leq Ch^{2t}.$$

Furthermore, let $u_{\mathcal{K},j} \in V_\mathcal{K}^k$ be a unit vector in $\ker(\mu_{h,j} I - T_\mathcal{K})$. Then, there is a unit vector $u_j \in \ker(\mu I - T) \subset G_\mu$ such that

$$(4.10) \qquad \|u_j - u_{\mathcal{K},j}\|_L \leq Ch^t.$$

Proof. Combining the results from Lemma 4.2 and Lemma 4.3 with Theorem 2.1 and Theorem 2.3 completes the proof. □

Remark 4.5 (Error estimate on eigenvalues). Since the eigenvalues λ and λ_h associated with (2.2) and (3.12), respectively, are such that $\lambda = \mu^{-1}$ and $\lambda_h = \mu_h^{-1}$, we infer that the same estimate as (4.9) holds true for the error between λ and λ_h.

Corollary 4.6 (Eigenfunction error estimate in H^1). *Let us drop the index j for simplicity from the eigenfunction u_j and the approximate eigenfunction $u_{\mathcal{K},j}$ and let us set $\hat{u}_h = (u_{\mathcal{K}}, Z_{\mathcal{F},0}(u_{\mathcal{K}}))$. Then the following holds true:*

$$(4.11) \qquad \hat{a}_h(\hat{u}_h - \hat{I}_h^k(u), \hat{u}_h - \hat{I}_h^k(u))^{\frac{1}{2}} \leq Ch^t.$$

Consequently, we have

$$(4.12) \qquad \left(\sum_{K \in \mathcal{K}} \|\nabla(u - p_K^{k+1}(\hat{u}_K))\|_{L^2(K)}^2 \right)^{\frac{1}{2}} \leq Ch^t.$$

Proof. We observe that

$$\lambda_h(u_{\mathcal{K}}, u)_L = \lambda_h(u_{\mathcal{K}}, \Pi_{\mathcal{K}}^k(u))_L = \lambda_h b(u_{\mathcal{K}}, \Pi_{\mathcal{K}}^k(u)) = a_{\mathcal{K}}(u_{\mathcal{K}}, \Pi_{\mathcal{K}}^k(u))$$
$$= \hat{a}_h((u_{\mathcal{K}}, Z_{\mathcal{F},0}(u_{\mathcal{K}})), (\Pi_{\mathcal{K}}^k(u), Z_{\mathcal{F},0}^\dagger(\Pi_{\mathcal{K}}^k(u))))$$
$$= \hat{a}_h((u_{\mathcal{K}}, Z_{\mathcal{F},0}(u_{\mathcal{K}})), (\Pi_{\mathcal{K}}^k(u), Z_{\mathcal{F},0}^\dagger(\Pi_{\mathcal{K}}^k(u))))$$
$$\quad + \hat{a}_h((u_{\mathcal{K}}, Z_{\mathcal{F},0}(u_{\mathcal{K}})), (0, \Pi_{\mathcal{F}}^k(u) - Z_{\mathcal{F},0}^\dagger(\Pi_{\mathcal{K}}^k(u))))$$
$$= \hat{a}_h(\hat{u}_h, \hat{I}_h^k(u)),$$

where we have used the definition of $\Pi_{\mathcal{K}}^k$ and (3.21) in the first line, the definition (3.18) of $\hat{a}_h$ in the second line, the property (3.16) of $Z_{\mathcal{F},0}$ in the third line, and the definition of $\hat{I}_h^k$ in the last line. Setting $\delta_u := \hat{a}_h(\hat{I}_h^k(u), \hat{I}_h^k(u)) - a(u, u)$ and recalling the normalization $\|u\|_L = \|u_{\mathcal{K}}\|_L = 1$, we infer that

$$\hat{a}_h(\hat{u}_h - \hat{I}_h^k(u), \hat{u}_h - \hat{I}_h^k(u))$$
$$= \hat{a}_h(\hat{u}_h, \hat{u}_h) - 2\hat{a}_h(\hat{u}_h, \hat{I}_h^k(u)) + \hat{a}_h(\hat{I}_h^k(u), \hat{I}_h^k(u))$$
$$= \lambda_h \|u_{\mathcal{K}}\|_L^2 - 2\lambda_h(u_{\mathcal{K}}, u)_L + \lambda_h \|u\|_L^2 - (\lambda_h - \lambda)\|u\|_L^2 + \delta_u$$
$$= \lambda_h \|u_{\mathcal{K}} - u\|_L^2 - \lambda_h + \lambda + \delta_u,$$

which is a generalization of the Pythagorean eigenvalue error identity (see [44]) in the HHO context. The bound (4.11) then follows from the bounds derived in Theorem 4.4 (see in particular the bound on $S_{2,2}$ therein to estimate δ_u). Finally, the bound (4.12) follows from the definition of the bilinear form $\hat{a}_h$, the triangle inequality, and the approximation properties of the elliptic projector. $\square$

Remark 4.7 (Optimal convergence). If $t = k + 1$, we recover a convergence of order h^{2k+2} for the eigenvalues and of order k^{k+1} for the eigenfunctions in the H^1-seminorm.

5. Numerical experiments

In this section, we first verify the error estimates from Section 4 for eigenvalues and smooth eigenfunctions approximated by the HHO method in 1D (unit interval) and in 2D (unit square). We then study the effect of varying the stabilization parameter and, in particular, we report superconvergence results for 1D uniform meshes when using a particular value of the stabilization parameter. We next consider in 2D the use of polygonal (hexagonal) meshes and we compare our results

TABLE 1. Unit interval, relative eigenvalue errors, $\eta = 1$.

k	N	first mode		second mode		fourth mode		eighth mode	
		error	order	error	order	error	order	error	order
	10	3.19e-2	—	1.17e-1	—	3.50e-1	—	6.99e-1	—
	20	8.16e-3	1.97	3.19e-2	1.87	1.17e-1	1.58	3.50e-1	1.00
0	40	2.05e-3	1.99	8.16e-3	1.97	3.19e-2	1.87	1.17e-1	1.58
	80	5.14e-4	2.00	2.05e-3	1.99	8.16e-3	1.97	3.19e-2	1.87
	160	1.28e-4	2.00	5.14e-4	2.00	2.05e-3	1.99	8.16e-3	1.97
	10	1.10e-4	—	1.81e-3	—	3.25e-2	—	4.01e-1	—
	20	6.78e-6	4.01	1.10e-4	4.05	1.81e-3	4.16	3.25e-2	3.63
1	40	4.23e-7	4.00	6.78e-6	4.01	1.10e-4	4.05	1.81e-3	4.16
	80	2.64e-8	4.00	4.23e-7	4.00	6.78e-6	4.01	1.10e-4	4.05
	160	1.65e-9	4.00	2.64e-8	4.00	4.23e-7	4.00	6.78e-6	4.01
	10	1.15e-7	—	7.52e-6	—	5.28e-4	—	6.08e-2	—
	20	1.79e-9	6.01	1.15e-7	6.03	7.52e-6	6.13	5.28e-4	6.85
2	40	2.78e-11	6.01	1.79e-9	6.01	1.15e-7	6.03	7.52e-6	6.13
	80	9.88e-14	8.14	2.78e-11	6.01	1.79e-9	6.01	1.15e-7	6.03

to those obtained using continuous finite elements. Finally, we present convergence results on an L-shaped domain (which includes the case of a non-smooth eigenfunction) and on the unit disk. In all cases, we consider the eigenvalues λ and λ_h associated with (2.2) and (3.12), respectively; both sets of eigenvalues are sorted in an increasing order as $\lambda_1 < \lambda_2 < \cdots$ and $\lambda_{1,h} < \lambda_{2,h} < \cdots$, and we report the normalized eigenvalue errors $\frac{|\lambda_j - \lambda_{h,j}|}{\lambda_j}$.

5.1. **Smooth eigenfunctions in 1D and 2D unit domains.** Let $\Omega = (0,1)$ or $\Omega = (0,1) \times (0,1)$ be the unit interval in 1D or the unit square in 2D, respectively. The 1D problem (2.1) has exact eigenvalues $\lambda_j = j^2 \pi^2$ and corresponding normalized eigenfunctions $u_j(x) = \sqrt{2} \sin(j\pi x)$ with $j = 1, 2, \ldots$, whereas the 2D problem (2.1) has exact eigenvalues $\lambda_{jk} = \pi^2 (j^2 + k^2)$ and normalized eigenfunctions $u_{jk}(x,y) = 2 \sin(j\pi x) \sin(k\pi y)$ with $j, k = 1, 2, \ldots$. We discretize the unit interval uniformly with $N \in \{10, 20, 40, 80, 160\}$ elements and the unit square uniformly with $N \times N$ squares with $N \in \{4, 8, 16, 32, 64\}$. The default stabilization parameter of the HHO method is $\eta = 1$. The relative eigenvalue errors are reported in Table 1 in 1D and in Table 2 in 2D for the first, second, fourth, and eighth eigenvalues and for the polynomial degrees $k \in \{0, 1, 2\}$. These tables show good agreement with the convergence order predicted by Theorem 4.4, i.e., the convergence order for the eigenvalues is indeed h^{2k+2}. The H^1-seminorm errors on the first, second, fourth, and eighth eigenfunctions in 1D are reported in Table 3. We observe a good agreement with the convergence order predicted by Corollary 4.6, that is, the convergence order for the eigenfunctions in the H^1-seminorm is indeed h^{k+1}.

TABLE 2. Unit square, relative eigenvalue errors, $\eta = 1$.

k	N	first mode		second mode		fourth mode		eighth mode	
		error	order	error	order	error	order	error	order
	4	2.51e-1	—	5.11e-1	—	6.36e-1	—	7.39e-1	—
	8	7.70e-2	1.70	2.16e-1	1.24	2.51e-1	1.34	4.08e-1	0.86
0	16	2.04e-2	1.92	6.57e-2	1.72	7.70e-2	1.70	1.33e-1	1.61
	32	5.18e-3	1.98	1.74e-2	1.92	2.04e-2	1.92	3.73e-2	1.84
	64	1.30e-3	1.99	4.41e-3	1.98	5.18e-3	1.98	9.62e-3	1.96
	4	2.27e-2	—	1.62e-1	—	3.32e-1	—	5.10e-1	—
	8	1.45e-3	3.97	9.75e-3	4.06	2.27e-2	3.87	6.35e-2	3.01
1	16	9.15e-5	3.98	5.96e-4	4.03	1.45e-3	3.97	3.90e-3	4.02
	32	5.74e-6	3.99	3.71e-5	4.00	9.15e-5	3.98	2.45e-4	3.99
	64	3.59e-7	4.00	2.32e-6	4.00	5.74e-6	3.99	1.54e-5	4.00
	4	5.71e-4	—	8.46e-3	—	4.91e-2	—	2.31e-1	—
	8	8.63e-6	6.05	1.07e-4	6.30	5.71e-4	6.43	2.33e-3	6.64
2	16	1.34e-7	6.01	1.62e-6	6.05	8.63e-6	6.05	3.34e-5	6.12
	32	2.09e-9	6.00	2.51e-8	6.01	1.34e-7	6.01	5.14e-7	6.02
	64	3.26e-11	6.00	3.92e-10	6.00	2.09e-9	6.00	8.01e-9	6.00

TABLE 3. Unit interval, H^1-seminorm errors on eigenfunctions, $\eta = 1$.

k	N	first mode		second mode		fourth mode		eighth mode	
		error	order	error	order	error	order	error	order
	10	2.08e-1	—	9.87e-1	—	4.39e0	—	1.61e+1	—
	20	1.02e-1	1.03	4.16e-1	1.25	1.97e0	1.15	8.78e0	0.88
0	40	5.05e-2	1.01	2.03e-1	1.03	8.32e-1	1.25	3.95e0	1.15
	80	2.52e-2	1.00	1.01e-1	1.01	4.06e-1	1.03	1.66e0	1.25
	160	1.26e-2	1.00	5.04e-2	1.00	2.02e-1	1.01	8.13e-1	1.03
	10	8.17e-3	—	9.87e-2	—	3.33e0	—	1.54e+1	—
	20	2.04e-3	2.00	1.63e-2	2.60	1.97e-1	4.08	6.67e0	1.21
1	40	5.11e-4	2.00	4.09e-3	2.00	3.27e-2	2.60	3.95e-1	4.08
	80	1.28e-4	2.00	1.02e-3	2.00	8.17e-3	2.00	6.53e-2	2.60
	160	3.19e-5	2.00	2.55e-4	2.00	2.04e-3	2.00	1.63e-2	2.00
	10	2.17e-4	—	4.36e-3	—	1.52e0	—	1.54e+1	—
	20	2.71e-5	3.00	4.34e-4	3.33	8.71e-3	7.45	3.05e0	2.33
2	40	3.39e-6	3.00	5.42e-5	3.00	8.67e-4	3.33	1.74e-2	7.45
	80	4.24e-7	3.00	6.78e-6	3.00	1.08e-4	3.00	1.73e-3	3.33
	160	5.30e-8	3.00	8.47e-7	3.00	1.36e-5	3.00	2.17e-4	3.00

TABLE 4. Unit interval, relative eigenvalue errors, $\eta = 2k + 3$.

k	N	first mode		second mode		fourth mode		eighth mode	
		error	order	error	order	error	order	error	order
	10	4.07e-5	—	6.59e-4	—	1.10e-2	—	1.80e-1	—
	20	2.54e-6	4.00	4.07e-5	4.02	6.59e-4	4.05	1.10e-2	4.04
0	40	1.59e-7	4.00	2.54e-6	4.00	4.07e-5	4.02	6.59e-4	4.05
	80	9.91e-9	4.00	1.59e-7	4.00	2.54e-6	4.00	4.07e-5	4.02
	160	6.19e-10	4.00	9.91e-9	4.00	1.59e-7	4.00	2.54e-6	4.00
	5	1.66e-6	—	1.13e-4	—	1.19e-2	—	1.74e-2	—
	10	2.55e-8	6.02	1.66e-6	6.09	1.13e-4	6.72	1.19e-2	0.54
1	20	3.98e-10	6.00	2.55e-8	6.02	1.66e-6	6.09	1.13e-4	6.72
	40	5.95e-12	6.06	3.98e-10	6.00	2.55e-8	6.02	1.66e-6	6.09
	4	9.18e-9	—	2.42e-6	—	1.34e-2	—	5.20e-1	—
2	8	3.57e-11	8.01	9.18e-9	8.04	2.42e-6	12.43	1.34e-2	5.28
	16	1.04e-13	8.42	3.57e-11	8.01	9.18e-9	8.04	2.42e-6	12.43

5.1.1. *Effect of the stabilization parameter η.* We first report some striking super-convergence results for the HHO method with the stabilization parameter set to $\eta = 2k + 3$ on 1D uniform meshes. In this case, we observe numerically two extra orders in the convergence of the relative eigenvalue errors, i.e., these errors now converge as h^{2k+4}; see Table 4. We thus obtain relative eigenvalue errors close to machine precision already on relatively coarse meshes. Moreover, we observe numerically (results are not reported for brevity) that taking values different from $2k + 3$ for the stabilization parameter does not improve the relative eigenvalue errors. We also point out that the choice $\eta = 2k+3$ does not increase the convergence order of the eigenfunctions. In 2D, we observe that the choice $\eta = 2k + 3$ improves the approximation significantly in the sense of a much smaller constant C in (4.9), but the convergence order remains h^{2k+2}. The results are reported in Table 5 (compare with Table 2). The theoretical analysis of the above observations is postponed to future work.

In all of our numerical experiments, the default choice $\eta = 1$ for the stabilization parameter produces satisfactory results. As expected, decreasing the value of η progressively leads to a loss of stability in the HHO stiffness matrix, and therefore to a degradation of the accuracy of the discrete eigenvalues and eigenfunctions. To illustrate this simple fact, we report in Table 6 the first four discrete eigenvalues using a polynomial degree $k \in \{0, 1, 2\}$ and a stabilization parameter $\eta = 2^{-l}$, $l \in \{0, \ldots, 6\}$. We consider here a quasi-uniform sequence of triangular meshes with an initial average mesh-size 0.017, where the next finer mesh in the sequence is produced by dividing each triangle into four congruent subtriangles. The results reported in Table 6 indicate that the sensitivity to the choice of a too small value of η swiftly decreases as the polynomial degree k increases. A similar study varying the stabilization parameter in the context of the VEM can be found in [40], where the loss of accuracy also follows from the loss of stability if the value assigned to the stabilization parameter is too low.

TABLE 5. Unit square, Relative eigenvalue errors, $\eta = 2k + 3$.

k	N	first mode		second mode		fourth mode		eighth mode	
		error	order	error	order	error	order	error	order
	4	4.23e-2	—	1.41e-1	—	1.66e-1	—	3.97e-1	—
	8	1.06e-2	1.99	3.60e-2	1.97	4.23e-2	1.97	7.84e-2	2.34
0	16	2.66e-3	2.00	9.04e-3	1.99	1.06e-2	1.99	1.98e-2	1.99
	32	6.65e-4	2.00	2.26e-3	2.00	2.66e-3	2.00	4.96e-3	2.00
	64	1.66e-4	2.00	5.66e-4	2.00	6.65e-4	2.00	1.24e-3	2.00
	4	2.74e-4	—	3.33e-3	—	5.80e-5	—	1.73e-2	—
	8	2.13e-5	3.69	1.69e-4	4.30	2.74e-4	-2.24	1.75e-4	6.63
1	16	1.40e-6	3.93	9.93e-6	4.09	2.13e-5	3.69	3.47e-6	5.66
	32	8.82e-8	3.98	6.11e-7	4.02	1.40e-6	3.93	4.41e-7	2.97
	64	5.53e-9	4.00	3.80e-8	4.01	8.82e-8	3.98	3.11e-8	3.83
	4	1.75e-5	—	3.33e-5	—	8.23e-4	—	1.28e-3	—
	8	2.90e-7	5.91	8.50e-7	5.29	1.75e-5	5.56	4.54e-5	4.82
2	16	4.60e-9	5.98	1.45e-8	5.87	2.90e-7	5.91	8.01e-7	5.82
	32	7.20e-11	6.00	2.32e-10	5.97	4.60e-9	5.98	1.29e-8	5.96
	64	2.66e-13	8.08	3.02e-12	6.26	7.20e-11	6.00	2.02e-10	5.99

TABLE 6. Discrete eigenvalues $\lambda_{h,j}$, $j \in \{1, 2, 3, 4\}$, with polynomial degree $k \in \{0, 1, 2\}$ and stabilization parameter $\eta = 2^{-l}$, $l \in \{0, \dots, 6\}$.

k	η	$\lambda_{h,1}$	$\lambda_{h,2}$	$\lambda_{h,3}$	$\lambda_{h,4}$
	1/4	1.74e1	3.70e1	3.73e1	5.11e1
0	1/2	1.85e1	4.25e1	4.27e1	6.26e1
	1	1.92e1	4.60e1	4.60e1	7.05e1
	1/64	1.57e1	5.09e1	5.11e1	8.16e1
1	1/8	1.97e1	4.87e1	4.87e1	7.54e1
	1	1.97e1	4.93e1	4.93e1	7.87e1
	1/64	1.97e1	4.94e1	4.94e1	7.90e1
2	1/8	1.97e1	4.93e1	4.93e1	7.89e1
	1	1.97e1	4.93e1	4.93e1	7.90e1

5.1.2. *Polygonal (hexagonal) meshes in 2D.* To illustrate the fact that the same convergence orders can be obtained if the HHO method is deployed on general meshes, we consider now a quasi-uniform sequence of polygonal (hexagonal) meshes of the unit square; see Figure 1. The coarsest mesh in the sequence is composed of predominantly hexagonal cells with average mesh-size 0.065; the average mesh-size is halved from one mesh in the sequence to the next finer mesh. Table 7 shows the relative eigenvalue errors for $k \in \{0, 1, 2\}$ with stabilization parameter $\eta = 1$
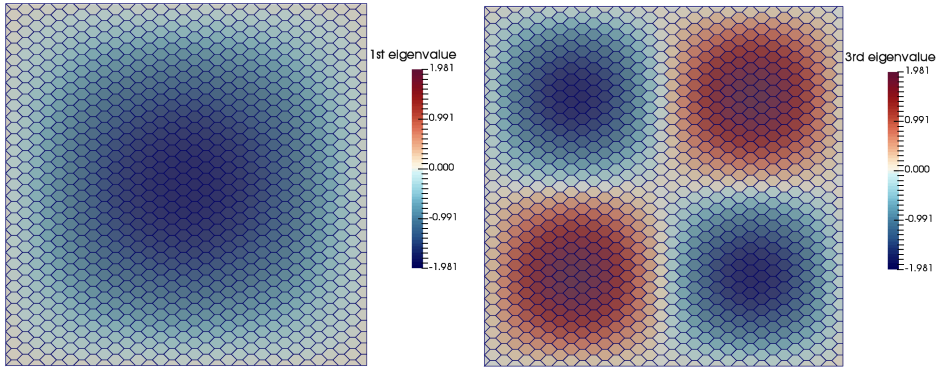
FIGURE 1. First and third approximate eigenfunctions with hexagonal meshes.

TABLE 7. Unit square with hexagonal meshes, relative eigenvalue errors, $\eta = 1$ and $\eta = 2k + 3$.

k	ℓ	$j = 1, \eta = 1$		$j = 1, \eta = 2k + 3$		$j = 3, \eta = 1$		$j = 3, \eta = 2k + 3$	
		error	order	error	order	error	order	error	order
0	0	3.20e-1	—	8.72e-2	—	6.69e-1	—	2.78e-1	—
	1	1.19e-1	1.43	2.21e-2	1.98	3.52e-1	0.93	8.41e-2	1.73
	2	3.56e-2	1.74	5.45e-3	2.02	1.28e-1	1.45	2.15e-2	1.97
	3	9.60e-3	1.89	1.35e-3	2.02	3.73e-2	1.78	5.37e-3	2.00
	4	2.48e-3	1.95	3.34e-4	2.01	9.84e-3	1.92	1.33e-3	2.01
1	0	1.97e-2	—	1.10e-3	—	3.16e-1	—	1.43e-2	—
	1	1.33e-3	3.89	8.28e-5	3.73	2.40e-2	3.72	1.32e-3	3.43
	2	8.74e-5	3.92	5.63e-6	3.88	1.45e-3	4.05	9.01e-5	3.88
	3	5.64e-6	3.95	3.66e-7	3.94	9.11e-5	3.99	5.86e-6	3.94
	4	3.59e-7	3.97	2.33e-8	3.97	5.75e-6	3.98	3.73e-7	3.97
2	0	2.99e-4	—	1.09e-5	—	4.09e-2	—	8.54e-4	—
	1	5.15e-6	5.86	2.26e-7	5.59	3.63e-4	6.82	1.42e-5	5.91
	2	8.55e-8	5.91	3.97e-9	5.83	5.59e-6	6.02	2.53e-7	5.81
	3	1.38e-9	5.95	6.52e-11	5.93	8.88e-8	5.98	4.17e-9	5.92
	4	2.21e-11	5.97	9.32e-13	6.13	1.41e-9	5.98	6.69e-11	5.96

and $\eta = 2k + 3$ for the first $(j = 1)$ and third $(j = 3)$ eigenpairs. We observe a convergence of order h^{2k+2}, in agreement with Theorem 4.4. Once again, the choice $\eta = 2k + 3$ for the stabilization parameter does not change the convergence order, but substantially improves the constant C.

5.1.3. *Comparison with the finite element method (FEM).* We now present a brief comparison between the discrete eigenvalues obtained using a continuous linear finite element method (FEM(1)) and the HHO method with $k = 0$ and $k = 1$

TABLE 8. Comparison of eigenvalue errors for $\lambda_{h,1}$ and $\lambda_{h,8}$ when using FEM(1), HHO(0) with $\eta = 1$ or $\eta = 8$, and HHO(1) with $\eta = 1$.

| ℓ | first eigenvalue | | | eighth eigenvalue | | | |
| | FEM(1) | HHO(0) | HHO(1) | FEM(1) | HHO(0) | | HHO(1) |
	- - -	$\eta = 1$	$\eta = 8$	$\eta = 1$	- - -	$\eta = 1$	$\eta = 8$	$\eta = 1$
0	1.75e-2	2.92e-2	9.72e-5	1.48e-4	1.15e-1	1.64e-1	2.76e-3	7.28e-3
1	4.36e-3	7.47e-3	2.57e-5	9.45e-6	2.79e-2	4.65e-2	8.48e-4	4.68e-4
2	1.09e-3	1.88e-3	6.81e-6	5.97e-7	6.94e-3	1.20e-2	2.21e-4	2.99e-5
3	2.72e-4	4.70e-4	1.75e-6	3.76e-8	1.73e-3	3.03e-3	5.59e-5	1.89e-6
4	6.81e-5	1.18e-4	4.40e-7	2.36e-9	4.33e-4	7.59e-4	1.40e-5	1.19e-7
ρ	2.00	1.99	1.95	3.99	2.01	1.95	1.92	3.98

(referred to as HHO(0) and HHO(1), respectively). We consider the same quasi-uniform sequence of triangular meshes as in Section 5.1.1, and we use the stabilization parameter $\eta = 1$ or $\eta = 8$ for HHO(0) and $\eta = 1$ for HHO(1). Table 8 reports the errors for the first and eighth eigenvalues. All the reported convergence orders (denoted as ρ in the table) match the theoretical predictions. HHO(0) with $\eta = 1$ leads to somewhat larger errors than FEM(1), but the situation is significantly reversed when using HHO(0) with $\eta = 8$ or HHO(1) with $\eta = 1$. We also mention that our numerical experiments show that the overall costs of FEM(1) and HHO(0) on various domains and mesh configurations are roughly the same.

5.2. **L-shaped domain.** We now study the Laplacian eigenvalue problem on the L-shaped domain $\Omega = \Omega_0 \backslash \Omega_1$, where $\Omega_0 = (0, 2) \times (0, 2)$ and $\Omega_1 = [1, 2] \times [1, 2]$. The L-shaped domain Ω has a re-entrant corner at the point $(1, 1)$, which results in possibly nonsmooth eigenfunctions. In fact, the first eigenfunction is in $H^{1+t}(\Omega)$ with $t = \frac{2}{3} - \epsilon$ with ϵ arbitrarily small, and the corresponding eigenvalue is $\lambda_1 = 9.6397238440219$ [7]. There are also smooth eigenfunctions. For example, the third eigenfunction is smooth and the corresponding eigenvalue is known exactly to be $\lambda_3 = 2\pi^2$. Figure 2 shows the HHO approximations (with $\eta = 1$) of the first and the third eigenfunctions using quasi-uniform triangulations of Ω and the polynomial degree $k = 1$.

To assess the convergence orders, we consider a sequence of triangulations where each of the three unit squares composing the L-shaped domain Ω is discretized uniformly with $2 \times N \times N$ triangular elements, where $N \in \{4, 8, 16, 32, 64\}$. Table 9 reports the relative eigenvalue errors for the first and third eigenvalues. We consider the values $\eta = 1$ and $\eta = 2k + 3$ for the stabilization parameter together with the polynomial degrees $k \in \{0, 1\}$. The relative error on the first eigenvalue converges with order h^{2t} with $2t \approx \frac{4}{3}$, whereas the relative error on the third eigenvalue converges with the optimal order h^{2k+2}. These results are again in agreement with Theorem 4.4. The errors with $\eta = 2k + 3$ are, as observed above, smaller than those with $\eta = 1$. Comparing with the results reported in [34] with HDG and $k = 0$, the HHO approximation of the first eigenvalue converges with order $h^{4/3}$ whereas the HDG approximation converges with order h; the HHO approximation

TABLE 9. L-shaped domain, relative eigenvalue errors, $\eta = 1$ and $\eta = 2k + 3$.

k	N	$j = 1, \eta = 1$		$j = 1, \eta = 2k + 3$		$j = 3, \eta = 1$		$j = 3, \eta = 2k + 3$	
		error	order	error	order	error	order	error	order
	4	2.36e-1	—	1.25e-1	—	3.60e-1	—	1.82e-1	—
	8	7.79e-2	1.60	4.12e-2	1.61	1.24e-1	1.54	5.32e-2	1.77
0	16	2.37e-2	1.72	1.37e-2	1.59	3.42e-2	1.86	1.39e-2	1.94
	32	7.32e-3	1.70	4.75e-3	1.53	8.77e-3	1.96	3.52e-3	1.98
	64	2.36e-3	1.63	1.71e-3	1.47	2.21e-3	1.99	8.82e-4	2.00
	4	2.08e-2	—	1.04e-2	—	2.24e-2	—	4.62e-3	—
	8	5.92e-3	1.81	4.12e-3	1.34	1.37e-3	4.04	2.77e-4	4.06
1	16	2.18e-3	1.44	1.64e-3	1.33	8.50e-5	4.01	1.72e-5	4.01
	32	8.55e-4	1.35	6.51e-4	1.33	5.31e-6	4.00	1.07e-6	4.00
	64	3.39e-4	1.34	2.58e-4	1.33	3.32e-7	4.00	6.71e-8	4.00
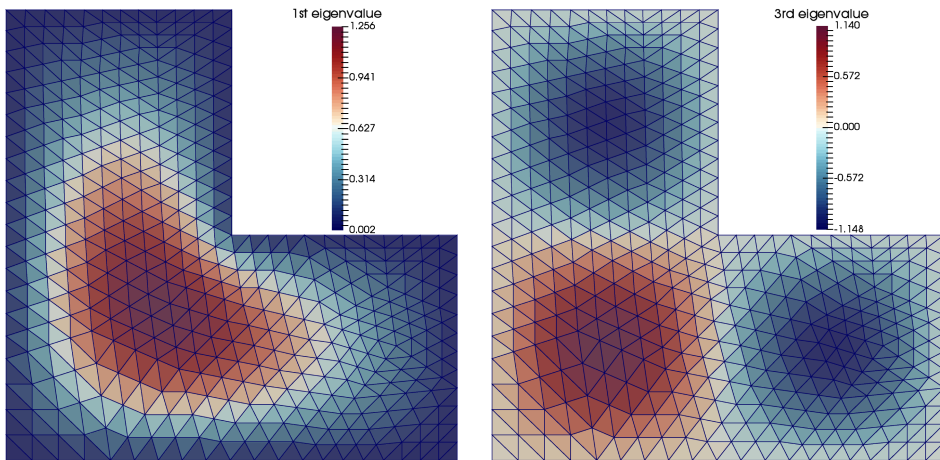
FIGURE 2. First and third approximate eigenfunctions in the L-shaped domain.

of the third eigenvalue converges with order h^2 whereas the HDG approximation converges with order h. Additionally, Table 10 shows the eigenfunction errors in the H^1-seminorm for the first and third modes. Here, the sequence of triangular meshes starts with an initial mesh-size 0.052, and the refinement procedure is the same as above. We use a linear FEM solution (normalized in $L^2(\Omega)$) solved at level 7 of the mesh sequence (this corresponds to a mesh-size 4.05×10^{-4}) as a reference solution for the calculation of the first eigenfunction error, and we use $u_3(x, y) = 2\sin(\pi x)\sin(\pi y)/\sqrt{3}$ (normalized in $L^2(\Omega)$) to compute the error on the third eigenfunction. In both cases, the error convergence rates are in good agreement with Theorem 4.4.

TABLE 10. L-shaped domain, first and third eigenfunction errors in the H^1-seminorm with polynomial degree $k \in \{0, 1\}$ and stabilization parameter $\eta \in \{1, 2k + 3\}$.

ℓ	first mode				third mode			
	$k = 0$		$k = 1$		$k = 0$		$k = 1$	
	$\eta = 1$	$\eta = 3$	$\eta = 1$	$\eta = 3$	$\eta = 1$	$\eta = 3$	$\eta = 1$	$\eta = 3$
0	1.38e0	1.33e0	3.80e-1	3.30e-1	2.36e0	2.16e0	4.73e-1	4.36e-1
1	7.42e-1	7.31e-1	2.21e-1	1.98e-1	1.20e0	1.14e0	1.09e-1	1.07e-1
2	4.09e-1	4.08e-1	1.40e-1	1.26e-1	5.88e-1	5.79e-1	2.68e-2	2.66e-2
3	2.34e-1	2.34e-1	9.09e-2	8.28e-2	2.92e-1	2.90e-1	6.65e-3	6.63e-3
4	1.39e-1	1.39e-1	6.18e-2	5.68e-2	1.46e-1	1.45e-1	1.62e-3	1.62e-3
order	0.83	0.81	0.65	0.63	1.01	0.98	2.04	2.01
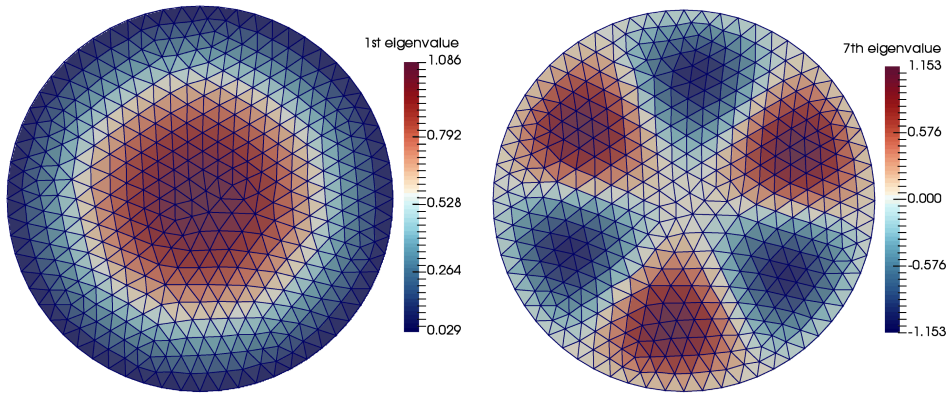
FIGURE 3. The first and seventh approximate eigenfunctions in the unit disk.

5.3. **Unit disk.** Lastly, we consider the Laplacian eigenvalue problem (2.1) in the unit disk $\Omega = \{(x, y) : x^2 + y^2 \leq 1\}$. Using polar coordinates, the eigenpairs are

$$(5.1) \quad (s_{n,m}^2, J_n(s_{n,m}r) \cos(n\theta))_{n=0,1,2,\ldots}, \qquad (s_{n,m}^2, J_n(s_{n,m}r) \sin(n\theta))_{n=1,2,\ldots},$$

where J_n is the Bessel function of order n, and $s_{n,m}$ are the zeros of the Bessel functions with $m = 1, 2, 3, \ldots$. Figure 3 shows the first and seventh discrete eigenfunctions.

We approximate the unit disk using a sequence of unstructured triangulations where the coarsest mesh in the sequence ($\ell = 0$) is composed of triangular cells with mesh-size 0.033, and the refinement procedure is the same as above. Since the boundary of the disk is approximated by straight lines, the error committed by this discretization is of order h^2. Thus, we only consider the lowest-order HHO approximation with $k = 0$. Table 11 reports the relative eigenvalue errors with $\eta = 2k + 3 = 3$ for the stabilization parameter. We observe a convergence order of h^2 as predicted.

TABLE 11. Unit disk, relative eigenvalue errors, $k = 0$ and $\eta = 3$.

k	ℓ	first mode		fourth mode		seventh mode	
		error	order	error	order	error	order
	0	6.35e-3	—	1.55e-2	—	3.19e-2	—
	1	1.59e-3	2.00	3.82e-3	2.02	7.95e-3	2.00
	2	3.98e-4	2.00	9.54e-4	2.00	1.99e-3	2.00
0	3	9.96e-5	2.00	2.38e-4	2.00	4.97e-4	2.00
	4	2.49e-5	2.00	5.96e-5	2.00	1.24e-4	2.00
	5	6.22e-6	2.00	1.49e-5	2.00	3.11e-5	2.00

6. Concluding remarks

In this paper, we devised and analyzed the approximation of the eigenvalues and eigenfunctions of a second-order selfadjoint elliptic operator using the Hybrid High-Order (HHO) method. Using polynomials of degree $k \geq 0$ for the face unknowns, and assuming smooth eigenfunctions, we established theoretically and observed numerically that the errors on the eigenvalues converge as h^{2k+2} whereas the errors on the eigenfunctions converge as h^{k+1} in the H^1-seminorm. We considered triangular and polygonal (hexagonal) meshes in the numerical experiments for the Laplace eigenproblem in two-dimensional domains with smooth and non-smooth eigenfunctions. Additionally, we observed numerically in one dimension that the eigenvalue error converges at the even faster rate h^{2k+4} for the particular choice $\eta = 2k + 3$ of the stabilization parameter in the HHO method. Several extensions of the present work can be considered, among which we mention biharmonic eigenvalue problems and non-selfadjoint second-order eigenvalue problems as well as the Maxwell eigenvalue problem in a curl-curl setting.

References

[1] M. Abbas, A. Ern, and N. Pignet, *Hybrid high-order methods for finite deformations of hyperelastic materials*, Comput. Mech. **62** (2018), no. 4, 909–928, DOI 10.1007/s00466-018-1538-0. MR3851857

[2] M. Ainsworth and H. A. Wajid, *Optimally blended spectral-finite element scheme for wave propagation and nonstandard reduced integration*, SIAM J. Numer. Anal. **48** (2010), no. 1, 346–371, DOI 10.1137/090754017. MR2644367

[3] P. F. Antonietti, A. Buffa, and I. Perugia, *Discontinuous Galerkin approximation of the Laplace eigenproblem*, Comput. Methods Appl. Mech. Engrg. **195** (2006), no. 25-28, 3483–3503, DOI 10.1016/j.cma.2005.06.023. MR2220929

[4] D. N. Arnold, *An interior penalty finite element method with discontinuous elements*, SIAM J. Numer. Anal. **19** (1982), no. 4, 742–760, DOI 10.1137/0719052. MR664882

[5] B. Ayuso de Dios, K. Lipnikov, and G. Manzini, *The nonconforming virtual element method*, ESAIM Math. Model. Numer. Anal. **50** (2016), no. 3, 879–904, DOI 10.1051/m2an/2015090. MR3507277

[6] I. Babuška and J. Osborn, *Eigenvalue problems*, Handbook of Numerical Analysis, Vol. II, Handb. Numer. Anal., II, North-Holland, Amsterdam, 1991, pp. 641–787. MR1115240

[7] T. Betcke and L. N. Trefethen, *Reviving the method of particular solutions*, SIAM Rev. **47** (2005), no. 3, 469–491, DOI 10.1137/S0036144503437336. MR2178637

[8] D. Boffi, *Finite element approximation of eigenvalue problems*, Acta Numer. **19** (2010), 1–120, DOI 10.1017/S0962492910000012. MR2652780

[9] D. Boffi, F. Brezzi, and L. Gastaldi, *On the problem of spurious eigenvalues in the approximation of linear elliptic problems in mixed form*, Math. Comp. **69** (2000), no. 229, 121–140, DOI 10.1090/S0025-5718-99-01072-8. MR1642801

[10] J. H. Bramble and J. E. Osborn, *Rate of convergence estimates for nonselfadjoint eigenvalue approximations*, Math. Comp. **27** (1973), 525–549, DOI 10.2307/2005658. MR0366029

[11] S. C. Brenner, *Poincaré-Friedrichs inequalities for piecewise H^1 functions*, SIAM J. Numer. Anal. **41** (2003), no. 1, 306–324, DOI 10.1137/S0036142902401311. MR1974504

[12] H. Brezis, *Functional Analysis, Sobolev Spaces and Partial Differential Equations*, Universitext, Springer, New York, 2011. MR2759829

[13] V. Calo, Q. Deng, and V. Puzyrev, *Dispersion optimized quadratures for isogeometric analysis*, arXiv:1702.04540 (2017).

[14] C. Canuto, *Eigenvalue approximations by mixed methods* (English, with French summary), RAIRO Anal. Numér. **12** (1978), no. 1, 27–50, iii, DOI 10.1051/m2an/1978120100271. MR0488712

[15] P. G. Ciarlet, *The Finite Element Method for Elliptic Problems*, Classics in Applied Mathematics, vol. 40, Society for Industrial and Applied Mathematics (SIAM), Philadelphia, PA, 2002. Reprint of the 1978 original [North-Holland, Amsterdam; MR0520174 (58 #25001)]. MR1930132

[16] M. Cicuttin, D. A. Di Pietro, and A. Ern, *Implementation of discontinuous skeletal methods on arbitrary-dimensional, polytopal meshes using generic programming*, J. Comput. Appl. Math. **344** (2018), 852–874, DOI 10.1016/j.cam.2017.09.017. MR3825556

[17] B. Cockburn, D. A. Di Pietro, and A. Ern, *Bridging the hybrid high-order and hybridizable discontinuous Galerkin methods*, ESAIM Math. Model. Numer. Anal. **50** (2016), no. 3, 635–650, DOI 10.1051/m2an/2015051. MR3507267

[18] B. Cockburn, J. Gopalakrishnan, and R. Lazarov, *Unified hybridization of discontinuous Galerkin, mixed, and continuous Galerkin methods for second order elliptic problems*, SIAM J. Numer. Anal. **47** (2009), no. 2, 1319–1365, DOI 10.1137/070706616. MR2485455

[19] B. Cockburn, J. Gopalakrishnan, F. Li, N.-C. Nguyen, and J. Peraire, *Hybridization and postprocessing techniques for mixed eigenfunctions*, SIAM J. Numer. Anal. **48** (2010), no. 3, 857–881, DOI 10.1137/090765894. MR2669393

[20] Q. Deng, M. Bartoň, V. Puzyrev, and V. Calo, *Dispersion-minimizing quadrature rules for C^1 quadratic isogeometric analysis*, Comput. Methods Appl. Mech. Engrg. **328** (2018), 554–564, DOI 10.1016/j.cma.2017.09.025. MR3726137

[21] Q. Deng and V. Calo, *Dispersion-minimized mass for isogeometric analysis*, Comput. Methods Appl. Mech. Engrg. **341** (2018), 71–92, DOI 10.1016/j.cma.2018.06.016. MR3845617

[22] J. Descloux, N. Nassif, and J. Rappaz, *On spectral approximation. I. The problem of convergence* (English, with French summary), RAIRO Anal. Numér. **12** (1978), no. 2, 97–112, iii, DOI 10.1051/m2an/1978120200971. MR0483400

[23] J. Descloux, N. Nassif, and J. Rappaz, *On spectral approximation. II. Error estimates for the Galerkin method* (English, with French summary), RAIRO Anal. Numér. **12** (1978), no. 2, 113–119, iii, DOI 10.1051/m2an/1978120201131. MR0483401

[24] D. A. Di Pietro and J. Droniou, *A hybrid high-order method for Leray-Lions elliptic equations on general meshes*, Math. Comp. **86** (2017), no. 307, 2159–2191, DOI 10.1090/mcom/3180. MR3647954

[25] D. A. Di Pietro, J. Droniou, and A. Ern, *A discontinuous-skeletal method for advection-diffusion-reaction on general meshes*, SIAM J. Numer. Anal. **53** (2015), no. 5, 2135–2157, DOI 10.1137/140993971. MR3395131

[26] D. A. Di Pietro and A. Ern, *Discrete functional analysis tools for discontinuous Galerkin methods with application to the incompressible Navier-Stokes equations*, Math. Comp. **79** (2010), no. 271, 1303–1330, DOI 10.1090/S0025-5718-10-02333-1. MR2629994

[27] D. A. Di Pietro and A. Ern, *A hybrid high-order locking-free method for linear elasticity on general meshes*, Comput. Methods Appl. Mech. Engrg. **283** (2015), 1–21, DOI 10.1016/j.cma.2014.09.009. MR3283758

[28] D. A. Di Pietro, A. Ern, and S. Lemaire, *An arbitrary-order and compact-stencil discretization of diffusion on general meshes based on local reconstruction operators*, Comput. Methods Appl. Math. **14** (2014), no. 4, 461–472, DOI 10.1515/cmam-2014-0018. MR3259024

[29] D. A. Di Pietro, A. Ern, A. Linke, and F. Schieweck, *A discontinuous skeletal method for the viscosity-dependent Stokes problem*, Comput. Methods Appl. Mech. Engrg. **306** (2016), 175–195, DOI 10.1016/j.cma.2016.03.033. MR3502564

[30] R. G. Durán, L. Gastaldi, and C. Padra, *A posteriori error estimators for mixed approximations of eigenvalue problems*, Math. Models Methods Appl. Sci. **9** (1999), no. 8, 1165–1178, DOI 10.1142/S021820259900052X. MR1722056

[31] F. Gardini, *Mixed approximation of eigenvalue problems: a superconvergence result*, M2AN Math. Model. Numer. Anal. **43** (2009), no. 5, 853–865, DOI 10.1051/m2an/2009005. MR2559736

[32] F. Gardini and G. Vacca, *Virtual element method for second-order elliptic eigenvalue problems*, IMA Journal of Numerical Analysis (2017), drx063.

[33] S. Giani, *hp-adaptive composite discontinuous Galerkin methods for elliptic eigenvalue problems on complicated domains*, Appl. Math. Comput. **267** (2015), 604–617, DOI 10.1016/j.amc.2015.01.031. MR3399075

[34] J. Gopalakrishnan, F. Li, N.-C. Nguyen, and J. Peraire, *Spectral approximations by the HDG method*, Math. Comp. **84** (2015), no. 293, 1037–1059, DOI 10.1090/S0025-5718-2014-02885-8. MR3315499

[35] P. Grisvard, *Elliptic Problems in Nonsmooth Domains*, Monographs and Studies in Mathematics, vol. 24, Pitman (Advanced Publishing Program), Boston, MA, 1985. MR775683

[36] T. J. R. Hughes, J. A. Evans, and A. Reali, *Finite element and NURBS approximations of eigenvalue, boundary-value, and initial-value problems*, Comput. Methods Appl. Mech. Engrg. **272** (2014), 290–320, DOI 10.1016/j.cma.2013.11.012. MR3171285

[37] F. Jochmann, *An H^s-regularity result for the gradient of solutions to elliptic equations with mixed boundary conditions*, J. Math. Anal. Appl. **238** (1999), no. 2, 429–450, DOI 10.1006/jmaa.1999.6518. MR1715492

[38] B. Mercier, J. Osborn, J. Rappaz, and P.-A. Raviart, *Eigenvalue approximation by mixed and hybrid methods*, Math. Comp. **36** (1981), no. 154, 427–453, DOI 10.2307/2007651. MR606505

[39] B. Mercier and J. Rappaz, *Eigenvalue approximation via non-conforming and hybrid finite element methods*, Publications des séminaires de mathématiques et informatique de Rennes **1978** (1978), no. S4, 1–16, Available at `http://www.numdam.org/item?id= PSMIR_1978___S4_A10_0`.

[40] D. Mora, G. Rivera, and R. Rodríguez, *A virtual element method for the Steklov eigenvalue problem*, Math. Models Methods Appl. Sci. **25** (2015), no. 8, 1421–1445, DOI 10.1142/S0218202515500372. MR3340705

[41] J. E. Osborn, *Spectral approximation for compact operators*, Math. Comput. **29** (1975), 712–725. MR0383117

[42] V. Puzyrev, Q. Deng, and V. Calo, *Dispersion-optimized quadrature rules for isogeometric analysis: modified inner products, their dispersion properties, and optimally blended schemes*, Comput. Methods Appl. Mech. Engrg. **320** (2017), 421–443, DOI 10.1016/j.cma.2017.03.029. MR3646360

[43] G. Savaré, *Regularity results for elliptic equations in Lipschitz domains*, J. Funct. Anal. **152** (1998), no. 1, 176–201, DOI 10.1006/jfan.1997.3158. MR1600081

[44] G. Strang and G. J. Fix, *An Analysis of the Finite Element Method*, Prentice-Hall Series in Automatic Computation, Prentice-Hall, Inc., Englewood Cliffs, N. J., 1973. MR0443377

[45] G. M. Vaĭnikko, *Asymptotic error bounds for projection methods in the eigenvalue problem* (Russian), Ž. Vyčisl. Mat. i Mat. Fiz. **4** (1964), 405–425. MR0176340

[46] G. M. Vaĭnikko, *Rapidity of convergence of approximation methods in eigenvalue problems* (Russian), Ž. Vyčisl. Mat. i Mat. Fiz. **7** (1967), 977–987. MR0221746

[47] J. Wang and X. Ye, *A weak Galerkin finite element method for second-order elliptic problems*, J. Comput. Appl. Math. **241** (2013), 103–115, DOI 10.1016/j.cam.2012.10.003. MR2994424

Department of Applied Geology, Western Australian School of Mines, Curtin University, Kent Street, Bentley, Perth, WA 6102, Australia; and Mineral Resources, Commonwealth Scientific and Industrial Research Organisation (CSIRO), Kensington, Perth, WA 6152, Australia
    Email address: `victor.calo@curtin.edu.au`

University Paris-Est, CERMICS (ENPC), 77455 Marne la Vallée cedex 2, and INRIA Paris, 75589 Paris, France
    Email address: `matteo.cicuttin@enpc.fr`

Curtin Institute for Computation and Department of Applied Geology, Western Australian School of Mines, Curtin University, Kent Street, Bentley, Perth, WA 6102, Australia
    Email address: `quanling.deng@curtin.edu.au`

University Paris-Est, CERMICS (ENPC), 77455 Marne la Vallée cedex 2, and INRIA Paris, 75589 Paris, France
    Email address: `alexandre.ern@enpc.fr`